

# Graphene-Based Nanomaterials in Photodynamic Therapy: Synthesis Strategies, Functional Roles, and Clinical Translation for Tumor Treatment

Junhan Liang<sup>1</sup>, Yang Wu<sup>2</sup>, Changyuan Zhang<sup>2</sup>, Ran Yi<sup>2</sup>, Jing Zheng<sup>2</sup>, Ruifen Zhao<sup>3</sup>, Dan Shan<sup>4</sup>, Baiqi Wang<sup>2,5-7</sup>

<sup>1</sup>School of Biomedical Engineering and Technology, Tianjin Medical University, Tianjin, 300070, People's Republic of China; <sup>2</sup>Department of Occupational and Environmental Health, School of Public Health, Tianjin Medical University, Tianjin, 300070, People's Republic of China; <sup>3</sup>Department of Safety Engineering, College of Chemical Engineering, Inner Mongolia University of Technology, Hohhot, 010051, People's Republic of China; <sup>4</sup>Department of Medical, Tianjin Stomatological Hospital, School of Medicine, Nankai University, Tianjin, 300041, People's Republic of China; <sup>5</sup>Key Laboratory of Prevention and Control of Major Diseases in the Population, Ministry of Education, Tianjin Medical University, Tianjin, 300070, People's Republic of China; <sup>6</sup>Tianjin Key Laboratory of Environment, Nutrition and Public Health, Tianjin, 300070, People's Republic of China; <sup>7</sup>National Demonstration Center for Experimental Preventive Medicine Education (Tianjin Medical University), Tianjin, 300070, People's Republic of China

Correspondence: Baiqi Wang, School of Public Health, Tianjin Medical University, Tianjin, 300070, People's Republic of China, Email wangbaiqi@tmu.edu.cn

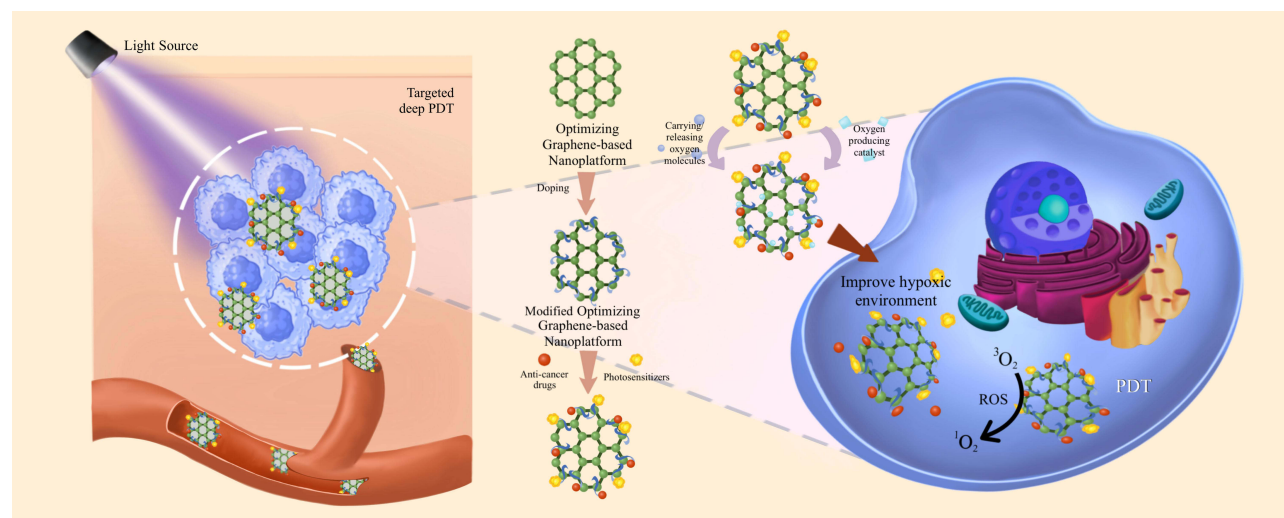
**Abstract:** Photodynamic therapy (PDT) is an effective approach for inducing tumor cell death through reactive oxygen species (ROS) generated by light-activated photosensitizers (PSs). Despite its selectivity in tumor treatment, PDT still faces significant challenges in targeting deep-seated tumors due to limitations in tissue penetration and precise localization. Graphene-based nanomaterials, such as graphene oxide (GO), reduced graphene oxide (rGO), graphene quantum dots (GQDs), and graphene nanosheets (GNS), offer innovative solutions by enhancing light penetration, boosting PS activity, and improving tumor-targeting precision. This review highlights how graphene-based nanomaterials address these challenges through functionalization strategies, including receptor-mediated tumor targeting, size-dependent penetration, optical synergy, and hypoxia modulation. Additionally, it explores the synthesis and production challenges associated with these materials. Focusing on four key graphene derivatives—GO, rGO, GQDs, and GNS—this article examines how reaction conditions, catalyst types, and precursor purity influence their structural properties and functional performance in PDT. To facilitate the translation from laboratory research to clinical application, strategies for scaling up production are discussed, emphasizing the need to simplify synthesis processes and improve efficiency for broader biomedical use. This review provides valuable insights into advancing graphene-based nanomaterials for clinical PDT applications, bridging the gap between nanomaterial design and therapeutic precision.

**Keywords:** graphene-based nanomaterials, photodynamic therapy, functionalization strategies, targeting, tumor therapy

## Introduction

Malignant tumors, more commonly known as cancer, pose a formidable threat to human health and are a significant public health challenge globally. The progression of cancer from a localized tumor to a metastatic disease is a sophisticated and multifaceted process, which remains the leading cause of death among cancer patients.<sup>1</sup> According to the latest projections from CA: A Cancer Journal for Clinicians,<sup>2</sup> an estimated 2,041,910 new cancer cases and 618,120 cancer-related deaths are expected to occur in the United States in 2025. These estimates are based on the most recent population-based cancer incidence data collected through 2021 and mortality data gathered through 2022. Despite significant advancements in anti-cancer treatments over the past decade, the battle against this relentless disease continues to be arduous. Currently, the primary clinical strategies for combating tumors include surgery, radiotherapy, chemotherapy, and immunotherapy. These methods have proven effective in curbing the proliferation of cancer cells. However, their lack of specificity often results in the inadvertent targeting of rapidly dividing normal cells, such as those in hair follicles, bone marrow, and the gastrointestinal tract, leading to substantial adverse effects.<sup>3</sup>

## Graphical Abstract



In this context, the development of new targeting strategies becomes crucial to strike a balance between treatment efficacy and the minimization of side effects. Photodynamic therapy (PDT) has emerged as a promising approach, leveraging photosensitizers (PSs) activation to generate cytotoxic singlet oxygen ( $^1O_2$ ) and reactive oxygen species (ROS) for tumor cell apoptosis.<sup>4</sup> It offers precise spatial control, allowing light exposure to be finely tuned for maximized effectiveness in tumor areas. Its non-invasiveness, controllability, reduced toxicity, and high efficiency make it a promising standalone or synergistic treatment option. However, conventional PSs often suffer from nonspecific accumulation in normal tissues, leading to off-target toxicity.<sup>5</sup> Additionally, light attenuation and hypoxia in deep tumors restrict ROS generation, thereby reducing therapeutic efficacy.<sup>6</sup> Ongoing advancements in light sources and light delivery technologies continue to underscore the pivotal role of appropriate PS selection in enhancing the tissue penetration of PDT, marking substantial progress in its application.

In the evolving domain of nanomedicine, graphene and its derivatives - including monolayer graphene, graphene oxide (GO), reduced graphene oxide (rGO), graphene quantum dots (GQDs), and graphene nanosheets (GNS) - have gained significant attention for their unique structural, chemical, and optical properties. Among their numerous applications, they have shown considerable promise in targeted drug delivery, bio-detection, bio-imaging, and phototherapy, including photo-thermal therapy (PTT) and PDT.<sup>7-10</sup> Specifically in PDT, these graphene-based nanomaterials are lauded for their broad-spectrum light absorption capabilities, which enable them to harness energy across a wide range of wavelengths. This quality not only boosts the excitation efficiency of PSs under targeted light conditions but also enhances the generation of  $^1O_2$  and ROS, crucial mediators in the therapeutic efficacy of PDT. Furthermore, graphene-based materials facilitate a more efficient transfer of light energy, reducing energy loss and non-radiative decay, thus amplifying the overall effectiveness of the PDT process. Beyond their optical advantages, graphene nanomaterials improve PDT by enhancing PS delivery, promoting tumor-selective accumulation, and mitigating tumor hypoxia through oxygen transport mechanisms. Their ability to encapsulate PSs prevents premature deactivation, improving treatment stability. Moreover, integrating graphene-based PDT with other therapeutic strategies holds promise for synergistic effects, potentially enhancing overall efficacy.

Despite the significant potential of these materials, there remains a notable gap in comprehensive reviews on the application of graphene in PDT, especially in the context of tumor treatment. This study aims to address this gap by reviewing recent advancements in graphene-based nanomaterials, focusing specifically on the synthesis and development of GO, rGO, GQDs, and GNS. It thoroughly examines the performance and therapeutic efficacy of these materials in PDT, offering insight into how they may overcome existing challenges and limitations in cancer therapy.

## Literature Search and Selection Methodology

To systematically review advancements in graphene-based nanomaterials for PDT in tumor treatment, a structured literature search strategy was implemented. First, a preliminary search was conducted in the PubMed database using the Boolean phrase “Nanomedicine AND Graphene AND Photodynamic Therapy AND Tumor AND Review” to identify relevant review articles published between 2020 and 2025, yielding 18 results. To broaden the scope, an ad hoc supplementary search was performed on Google Scholar, which identified additional reviews. These reviews provide in-depth discussions on specific topics, such as the synthesis and modification strategies of GO or rGO, and PDT combination therapies. A detailed review revealed that they typically focus on a single material type or address only particular aspects, such as drug delivery or imaging analysis. There is a notable gap in the systematic evaluation of the targeting accuracy and tissue penetration enhancement mechanisms of the four primary graphene-based materials—GO, rGO, GQDs, and GNS in PDT. Furthermore, these reviews lack a comprehensive analysis of the clinical feasibility and safety of these materials.

Subsequently, a comprehensive systematic review was conducted across four databases: ScienceDirect, PubMed, Web of Science and Scopus. This review used the predefined search string “Nanomedicine AND Graphene AND Photodynamic Therapy AND Tumor AND NOT Review” to identify original research articles published from 2020 to 2024.

Inclusion criteria encompassed:

1. Studies focusing on graphene-based nanomaterials for tumor-targeted PDT applications with demonstrated enhanced tumor-targeting precision or improved tissue penetration;
2. Experimental or preclinical research with robust data;
3. Studies that introduced innovative structural designs or functionalization strategies for graphene-based nanomaterials to enhance PDT performance.

Exclusion criteria were:

1. Non-primary research (eg, reviews, conference abstracts);
2. Studies unrelated to graphene-based nanomaterials, PDT, or tumor therapy;
3. Duplicate publications or incomplete datasets.

Review provides an in-depth analysis of studies that meet the aforementioned screening criteria. These articles form the core of the review, representing the most relevant studies, while additional references may also be cited to support broader context and trends. The search was focused on the period from 2020 to 2024. This was due to significant breakthroughs in the surface functionalization of graphene-based nanomaterials over the past five years, including targeting ligand conjugation and optimized PS loading, which have greatly enhanced their tumor-selective accumulation capabilities.

By examining research over the past decade and analyzing the key advancements in graphene-based PDT applications, we observe a notable increase in studies emphasizing enhanced targeting precision and improved tissue penetration strategies since 2020. This rising trend is anticipated to continue as more research integrates multimodal therapies and advanced bioengineered graphene nanocarriers to achieve superior tumor-specific delivery and deeper light penetration in PDT. The following sections provide a detailed breakdown of various functional modifications of graphene-based nanomaterials and their specific contributions to targeting precision and tissue penetration, ultimately enhancing PDT efficacy.

## Synthesis of Graphene-Based Nanomaterials in Photodynamic Therapy

The synthesis of graphene from carbon atoms is achieved through the process depicted in Figure 1, involving the formation of a covalent  $sp^2$  bond with a single-free electron.<sup>12</sup> The structure of graphene—consisting of a single, densely packed layer of carbon atoms—yields a specific surface area as high as  $2600 \text{ m}^2/\text{g}$ ,<sup>13</sup> vastly surpassing that of microporous activated carbon,

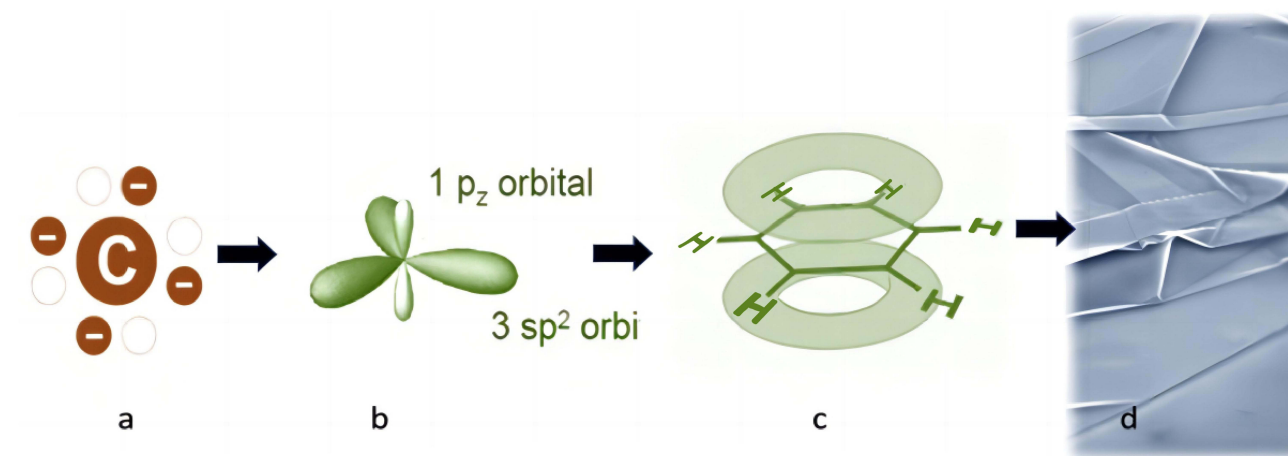


**Figure 1** (a–c) graphene bonding properties and (d) scanning electron microscope (SEM) image of single-layer graphene. Reprinted from Tiwari SK, Sahoo S, Wang N, Huczko A. Graphene research and their outputs: status and prospect. *J Sci.* 2020;5:10–29.<sup>11</sup>

which has a specific surface area ranging from 718 to 1591 m<sup>2</sup>/g.<sup>14</sup> This large surface area provides ample opportunities for modification and functionalization, making graphene an ideal platform for carrying PSs in PDT.

Graphene can be synthesized using various methods, which generally fall into two categories:

1. Redox Method: This method involves the oxidation of graphite to introduce oxygen-containing functional groups, followed by reduction to obtain graphene. This approach is favored for its simplicity and cost-effectiveness, making it suitable for industrial production. However, it typically results in a lower yield of graphene.<sup>11</sup>
2. Non-Redox Methods: These include techniques such as tape stripping, ultrasonic stripping with organic solvents, and electrochemical stripping. Although these methods produce higher-quality graphene, they tend to be more expensive and less efficient compared to the redox method.<sup>15</sup> The choice of graphene preparation method depends on specific requirements, considering factors such as cost, efficiency, and final product quality.

However, graphene's lack of a bandgap and poor water solubility limit its biomedical applications. To address these challenges, researchers are exploring the development of graphene derivatives. These derivatives aim to enhance the material's solubility, stability, and functionality, thereby broadening its applicability in biomedical fields, including PDT.<sup>16</sup>

## Synthesis of Graphene-Based Nanomaterials

### Preparation of GO

To provide a thorough understanding of GO synthesis, this section explores both traditional and modern methodologies, tracing their evolution over time. Traditional methods, such as those developed by Brodie and Hummers, established the foundational approaches for GO synthesis, though they came with safety and scalability challenges. In contrast, contemporary techniques, like the Tour method and its advancements, have refined these earlier methods by enhancing efficiency, safety, and product quality. Both traditional and modern approaches are vital in optimizing GO synthesis for large-scale production and diverse applications.

#### Traditional Synthesis Methods

British chemist B.C. Brodie pioneered the investigation into GO properties. In the Brodie method, graphite was combined with potassium chlorate (KClO<sub>3</sub>) in a 1:3 ratio and reacted with fuming nitric acid (HNO<sub>3</sub>) at 60°C for 3 to 4 days to produce GO.<sup>17</sup> This was the earliest method for preparing GO,<sup>18</sup> though the use of KClO<sub>3</sub> introduced a significant risk: the formation of chlorine dioxide (ClO<sub>2</sub>), a compound with explosive potential.

In 1958, Hummers and Offeman developed an alternative approach, known as the Hummers method,<sup>19</sup> which has since become one of the most widely used and effective techniques.<sup>20</sup> This method employs excess potassium permanganate



(KMnO<sub>4</sub>), sulfuric acid (H<sub>2</sub>SO<sub>4</sub>), and a small amount of sodium nitrate (NaNO<sub>3</sub>) to synthesize GO rapidly, typically within 8 to 12 hours. The combination of KMnO<sub>4</sub> and NaNO<sub>3</sub> results in a more ordered GO structure, enhancing its water solubility and ease of lamination.<sup>19</sup> One of the key advantages of the Hummers method is the replacement of KClO<sub>3</sub> with KMnO<sub>4</sub>, which mitigates the risk of explosive ClO<sub>2</sub> formation, thus improving safety. However, this method has its drawbacks, including the release of nitrogen oxides, which contribute to air pollution, and challenges in removing Na<sup>+</sup> and NO<sub>3</sub><sup>-</sup> from the final product.<sup>21</sup> Additionally, manganese heptoxide (Mn<sub>2</sub>O<sub>7</sub>), a highly explosive substance posing significant safety risks, may form inadvertently during the process. Specifically, Mn<sub>2</sub>O<sub>7</sub> is synthesized when solid potassium permanganate reacts with cold concentrated sulfuric acid, initially forming permanganic acid (HMnO<sub>4</sub>) that subsequently dehydrates to Mn<sub>2</sub>O<sub>7</sub>. Critically, Mn<sub>2</sub>O<sub>7</sub> decomposes explosively when heated to 55 °C,<sup>22</sup> which severely limits the process scalability due to thermal instability under practical operating conditions.

In 1999, Nina et al<sup>23</sup> introduced a pre-oxidation step to enhance the synthesis process. This method involved pre-oxidizing graphite with a mixture of H<sub>2</sub>SO<sub>4</sub>, potassium peroxodisulfate (K<sub>2</sub>S<sub>2</sub>O<sub>8</sub>), and phosphorus pentoxide (P<sub>2</sub>O<sub>5</sub>) at 80°C, followed by the synthesis of GO using the Hummers method. This modification accelerated the oxidation rate, resulting in a higher degree of oxidation in the produced GO.

In 2017, NI Zaaba and collaborators<sup>24</sup> further advanced GO synthesis by refining the Hummers method. Their improved technique removed the need for NaNO<sub>3</sub> and an ice bath, allowing the reaction to proceed at room temperature. This innovation demonstrated that NaNO<sub>3</sub> is not essential for GO synthesis, and GO with comparable properties can be produced without it. The revised method reduces costs and minimizes the emission of toxic gases, representing a significant improvement in the scalability and safety of GO production.

In 2022, Chen Xiaodong et al<sup>25</sup> conducted an in-depth study on the Hummers method for the preparation of GO, detailing a four-stage process. Initially, concentrated sulfuric and nitric acids infiltrate the graphite layers through molecular thermal motion, forming a HNO<sub>3</sub>-H<sub>2</sub>SO<sub>4</sub>-graphite intercalation compound (GIC). Subsequently, potassium permanganate reacts with sulfuric acid at low temperatures, generating Mn<sub>2</sub>O<sub>7</sub>. This Mn<sub>2</sub>O<sub>7</sub> then intercalates between the graphite layers, displacing some sulfuric acid molecules to form Mn<sub>2</sub>O<sub>7</sub>-H<sub>2</sub>SO<sub>4</sub>-GIC. In the third stage, Mn<sub>2</sub>O<sub>7</sub> decomposes thermally to produce oxygen atoms that oxidize the defects in the graphite layers, resulting in the formation of partially oxidized graphite oxide (PGO). Finally, the GO is purified using deionized water, hydrogen peroxide, and hydrochloric acid. This study offers a refined explanation of the oxidation mechanism involved in the Mn<sub>2</sub>O<sub>7</sub>-H<sub>2</sub>SO<sub>4</sub> oxidation method for GO preparation.

### Modern Synthesis Methods

**Tour's Graphene Oxide (TO-GO) Method:** In 2010, Dimiev and Tour introduced improvements to the Hummers method by substituting nitric acid with slightly corrosive phosphoric acid.<sup>26,27</sup> Their process involves mixing phosphoric and sulfuric acids in a 1:9 ratio, adding potassium permanganate and graphite in a 6:1 ratio in an ice bath, and then heating and stirring the mixture at 50°C for 12 hours. This modification enhances oxidation efficiency and product quality. After cooling the mixture, it is poured onto ice, and 30% hydrogen peroxide (H<sub>2</sub>O<sub>2</sub>) is added to neutralize any excess potassium permanganate, as depicted in Figure 2.<sup>28</sup> Phosphoric acid serves as a dispersant and etchant while stabilizing the oxidation process, thereby facilitating safer synthesis of GO. This method improves temperature control, avoids exothermic reactions, and mitigates the release of toxic gases, making it suitable for large-scale production.<sup>29</sup> The GO produced by this method exhibits higher yield, greater oxidation levels, and a more uniform structure compared to the Hummers method, with improved hydrophilicity and reduced defect concentration.<sup>30</sup>

In 2021, V.O. Kotsyubynsky et al<sup>31</sup> further refined the Tour method to produce a GO colloidal solution. By adding sodium hydroxide (NaOH) to adjust the pH to 2.0–2.2 in the final oxidation stage, they induced additional fragmentation of multilayer graphene particles, which were approximately 7.5 nanometers thick and consisted of 9–10 graphene layers. This increase in electrostatic repulsion between graphene particles enhanced the adsorption of hydroxide anions (OH<sup>-</sup>), resulting in improved colloidal stability and oxidation efficiency of the GO.

Beyond the Hummers and Tour methods, several other techniques such as Hofmann, Ruess, Scholz-Boehm, Nakajima-Matsuo, Lerf-Klinowski, and Dekany methods also produce GO with varying structures and properties tailored for diverse applications, as shown in Figure 3.<sup>32</sup> The choice of oxidizing agents plays a crucial role in determining the structure of GO,

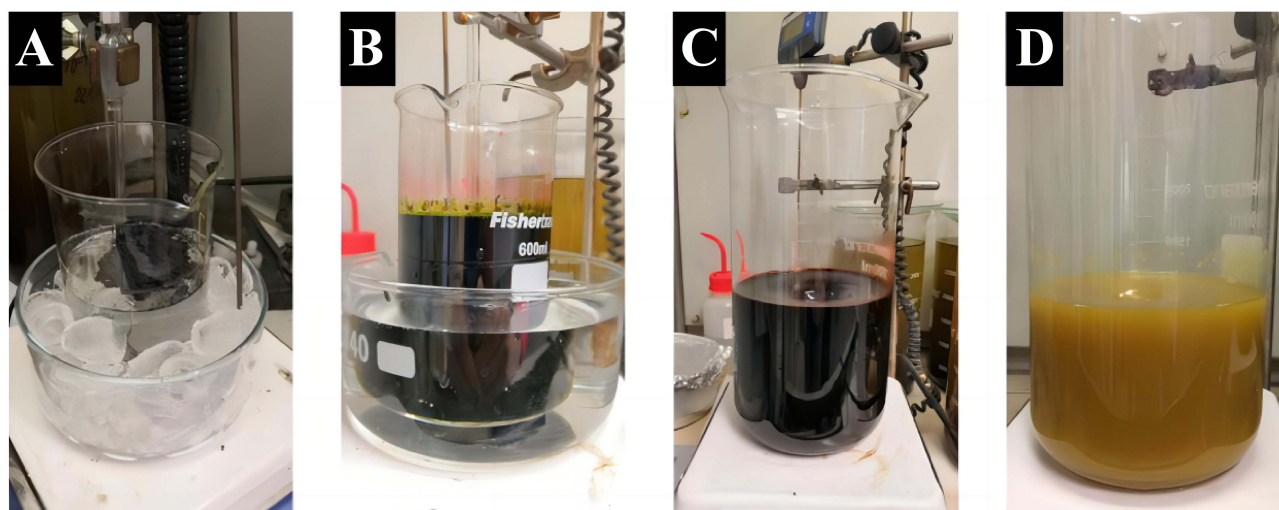


**Figure 2** Photographs describing preparation process of GO by Tour's method: (A) before addition of potassium permanganate; (B) after oxidation; (C) after pouring on ice; (D) after addition of  $\text{H}_2\text{O}_2$ . Reprinted from Jiříčková A, Jankovský O, Sofer Z, Sedmidubský D. Synthesis and Applications of Graphene Oxide. Materials. 2022;15(3):920. Under Creative Common CC BY license.<sup>28</sup>

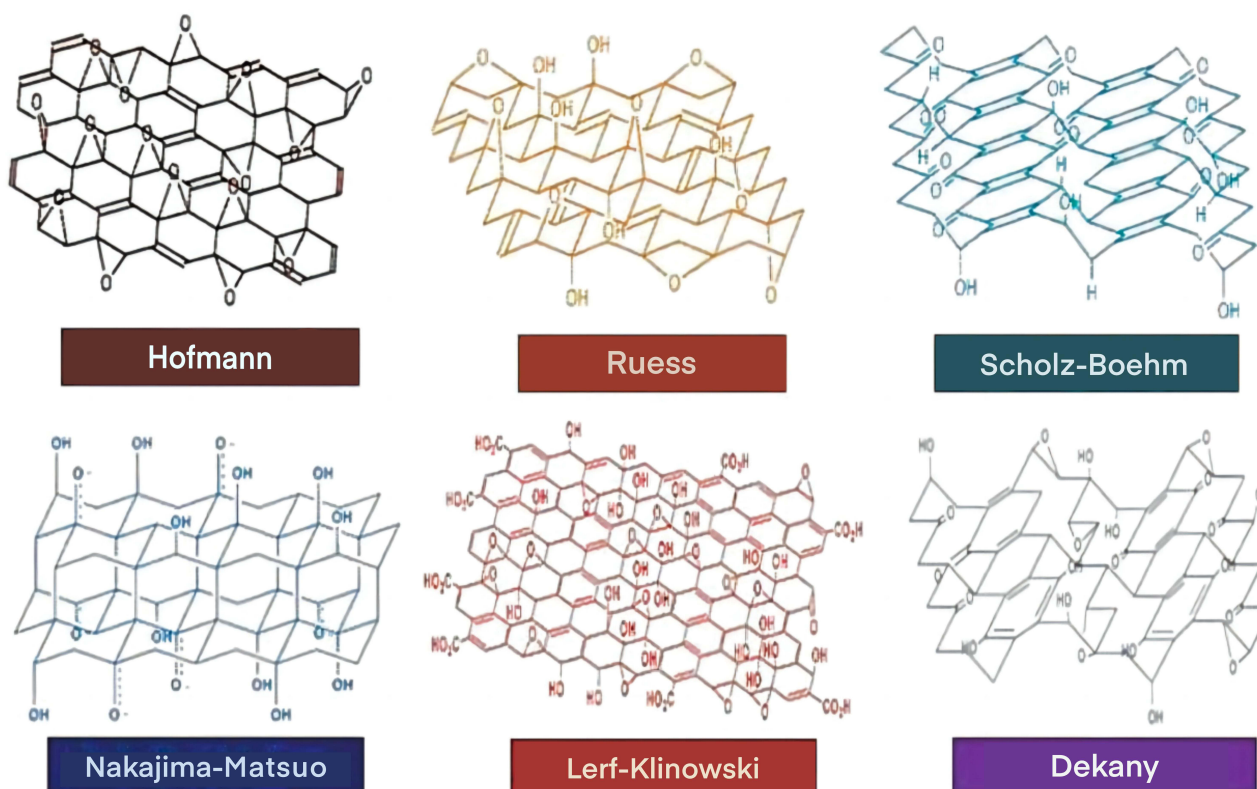


**Figure 3** Structure of graphene oxide obtained by different synthesis methods. Reproduced from Khan ZU, Kausar A, Ullah H, Badshah A, Khan WU. A review of graphene oxide, graphene buckypaper, and polymer/graphene composites: properties and fabrication techniques. J Plast Film Sheeting. 2016;32(4):336–379. doi:10.1177/8756087915614612. Sage is the original publisher of this figure.<sup>32</sup>

making the exploration of oxidation and exfoliation mechanisms vital for practical applications. The objective is to achieve a moderate degree of oxidation that allows for full exfoliation into single layers while maintaining the integrity of the carbon framework as much as possible.<sup>29</sup> Oxides obtained through different methods exhibit distinct structures and properties, making them suitable for various applications.<sup>32</sup>

## Preparation of rGO

1. Chemical Reduction Method: rGO is synthesized from GO through chemical reduction or heat treatment.<sup>34</sup> The chemical reduction process, illustrated in Figure 4,<sup>33</sup> involves the use of reducing agents like hydrazine hydrate ( $\text{N}_2\text{H}_4 \cdot \text{H}_2\text{O}$ ) or other alternatives. This method is cost-effective and can be performed at room temperature or under mild heating conditions. The reduction typically takes place in an electrochemical cell with a buffered aqueous solution. GO, after being stripped by ultrasound, is reduced for 2 hours using  $\text{N}_2\text{H}_4 \cdot \text{H}_2\text{O}$  to yield rGO.

Stankovich et al<sup>35</sup> were pioneers in using  $\text{N}_2\text{H}_4 \cdot \text{H}_2\text{O}$  as a reducing agent, appreciated for its water resistance, which facilitates its role as a dispersing solvent during the reduction process. The reaction mechanism resembles that of alkene reduction by  $\text{N}_2\text{H}_4$ .<sup>36</sup> However, due to the hazardous nature of  $\text{N}_2\text{H}_4$ , alternative reducing agents are employed. Sodium borohydride ( $\text{NaBH}_4$ ), ascorbic acid, and iodine (HI) serve as safer options. Ascorbic acid, in particular, is crucial for large-scale rGO production. It reduces Mn(VII) ions to Mn(II), causing GO's color to shift from yellow-green to black. The reduction leads to the loss of rGO's hydrophilicity, causing precipitation upon cooling, which is then filtered and freeze-dried to obtain rGO. This method is advantageous as it does not produce toxic gases.<sup>37</sup>

With increasing focus on green chemistry, alternative methods for rGO synthesis using natural materials and chemicals are gaining attention. Potential green reducing agents include metals like iron, zinc, and aluminum,<sup>38–40</sup> alkaline solutions such as sodium and potassium hydroxides,<sup>41</sup> phenols like gallic acid,<sup>42</sup> alcohols,<sup>43</sup> sugars,<sup>44</sup> microorganisms, and substances like glycine and vitamin C.<sup>45</sup> Despite their potential, these alternatives often introduce impurities or require harsh conditions, limiting their practical application.<sup>46</sup> Notably, caffeic acid (CA), a phenolic compound, has emerged as an eco-friendly and

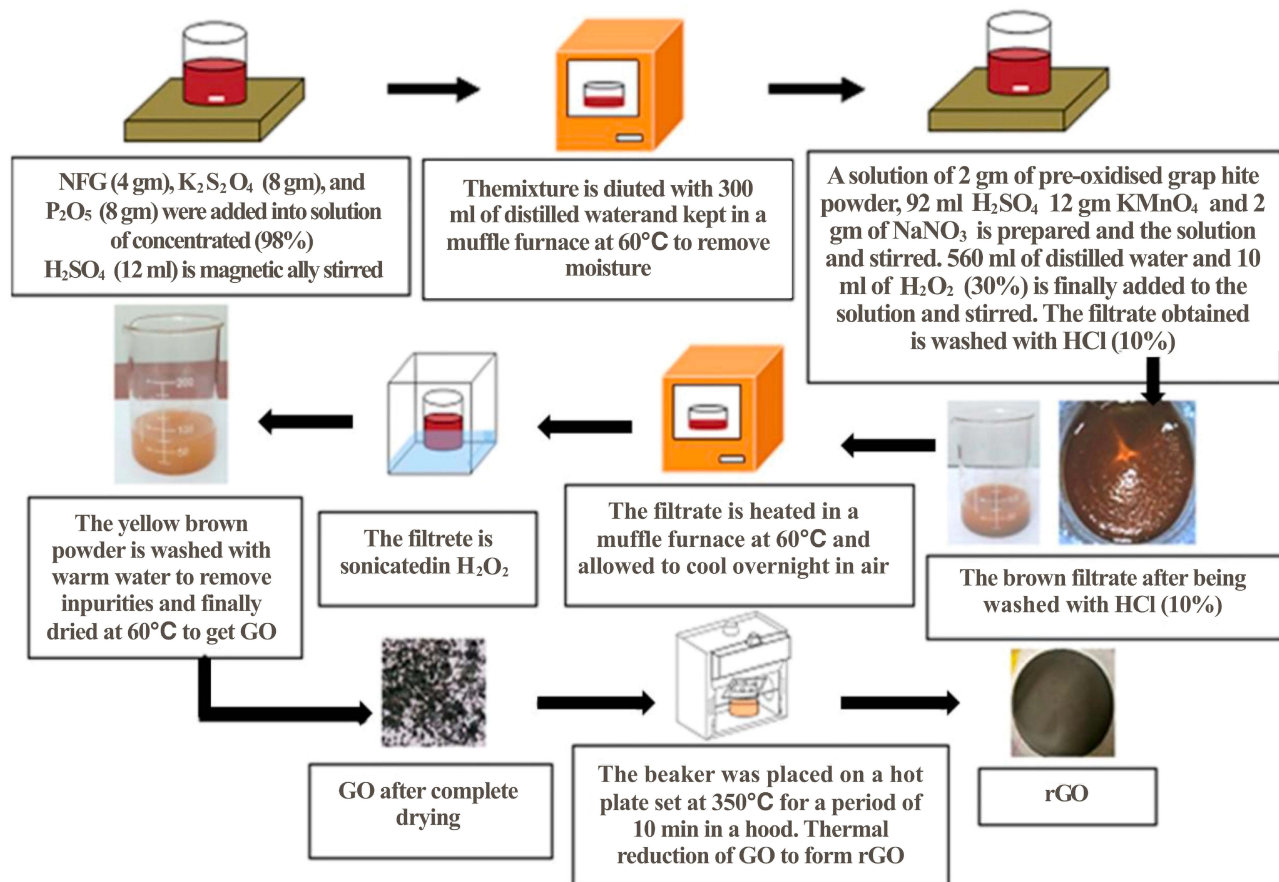


**Figure 4** The route of rGO synthesis by chemical reduction method. Reproduced from Alam N, Sharma N, Kumar L. Synthesis of Graphene Oxide (GO) by Modified Hummers Method and Its Thermal Reduction to Obtain Reduced Graphene Oxide (rGO) \* Open Access. Graphene. 2017;6(01):1–18. Under CC BY 4.0 <https://creativecommons.org/licenses/by/4.0/>.<sup>33</sup>

efficient reducing agent.<sup>46</sup> rGO produced with CA exhibits a high C/O ratio (7.15) and demonstrates exceptional performance in applications such as electronic gas sensors and supercapacitors, showing rapid response to NO<sub>2</sub> and NH<sub>3</sub> and high specific capacitance. This suggests that CA not only offers high reduction efficiency with minimal residual impurities but also boasts advantages such as low cost, environmental friendliness, and suitability for scalable production.

1. Thermal reduction method: Compared to chemical reduction, the thermal reduction method for preparing rGO has the notable advantage of not leaving harmful residues.<sup>36</sup> This process involves the thermal elimination of oxygen functional groups, resulting in the release of CO or CO<sub>2</sub> gases and the separation of the graphene/GO layers.<sup>34</sup> High-quality rGO with excellent electrical conductivity can be obtained through rapid annealing at temperatures as high as 1100°C. Despite its benefits, this method typically requires prolonged high-temperature treatment under protective gases like nitrogen (N<sub>2</sub>) or Ar. The energy-intensive nature of this process and the evolution of oxygen functional groups during reduction can lead to surface defects, such as nanoscale holes from carbon loss and Stone-Wales defects from carbon atom rearrangement. Additionally, the stable ether and carbonyl groups that form between the oxygen functional groups can hinder the reduction efficiency.<sup>47</sup> Recent advancements, including microwave<sup>47</sup> and photo-assisted thermal reduction methods,<sup>48</sup> have emerged to enhance the reduction efficiency by generating ultra-high temperature hot spots that promote the removal of oxygen groups and recovery of graphene structures.<sup>49</sup>
2. Electrochemical Reduction Method: Electrochemical reduction is an innovative technique for producing rGO, accomplished through electron exchange between the electrode and GO.<sup>50</sup> This method, producing electrochemically reduced graphene oxide (ERGO), is particularly attractive for fabricating GO-modified electrodes.<sup>51</sup> The absence of external reducing agents in electrochemical reduction means that ERGO is free from external contamination. By adjusting the applied potential, the degree of GO reduction can be controlled, allowing for selective removal of specific oxygen-containing groups.<sup>52</sup> This feature not only makes electrochemical reduction an environmentally friendly method but also enables the production of various ERGO coatings, such as porous networks or dense films.<sup>53</sup> The simplicity and mild reaction conditions of electrochemical reduction—without the need for high temperatures or pressures—make it a practical option for industrial applications. Furthermore, electrochemical reduction can be combined with other methods, such as adjusting the composition of the electrolyte or electrode materials, to tailor the properties of ERGO to specific requirements. Beyond structural and procedural distinctions, specific synthesis routes impart functional features to rGO that directly influence its photodynamic performance. For example, chemical reduction using N<sub>2</sub>H<sub>4</sub>·H<sub>2</sub>O often results in residual nitrogen dopants, which can enhance electron mobility and promote ROS generation under light irradiation.<sup>54</sup> Likewise, thermally reduced rGO typically exhibits defect-rich surfaces, which facilitate  $\pi$ - $\pi$  stacking interactions with PSs,<sup>55</sup> thereby improving drug loading capacity and tumor cell uptake. Although these synthesis-application correlations are not detailed in synthetic protocols, they are integral to the rational design of rGO-based PDT platforms and are further explored in later application-focused sections.

## Preparation of Graphene Quantum Dots

GQDs can be prepared using two main approaches: the top-down method and the bottom-up method.

### Top-Down Method

1. Chemical Oxidation Method: This widely-used method involves strong oxidants such as KClO<sub>3</sub> and KMnO<sub>4</sub>, along with acids like H<sub>2</sub>SO<sub>4</sub> and HNO<sub>3</sub>, to cleave carbon bonds in materials such as graphene, GO, or carbon nanotubes.<sup>56</sup> This process effectively oxidizes and fragments carbon precursors into nanoscale GO fragments, which are then reduced and stabilized into GQDs.<sup>57</sup> Although this method is cost-effective and suitable for large-scale production, it presents challenges such as the difficulty in removing by-products, which can negatively impact environmental sustainability.<sup>58</sup> The use of aggressive chemicals also introduces safety concerns and potential increases in production costs, necessitating careful waste management and optimization of reaction conditions to mitigate environmental impact and enhance efficiency.



2. **Ultrasound-Assisted Method:** This technique uses ultrasonic waves to create bubbles in a liquid medium that generate forces capable of breaking carbon-carbon bonds, thereby producing GQDs. The liquid medium typically consists of organic solvents such as N-methyl-2-pyrrolidone (NMP), dimethylformamide (DMF),  $\gamma$ -butyrolactone (GBL), 1,3-dimethyl-2-imidazolidinone (DMEU), isopropanol (IPA), or tetrahydrofuran (THF).<sup>59–61</sup> These solvents play a critical role in stabilizing the dispersed graphene sheets by modulating the liquid-phase surface tension, preventing reaggregation during ultrasonication. While water and ethanol alone are generally ineffective for graphene dispersion,<sup>62</sup> blending them with other solvents can optimize dispersion conditions, enabling a stable suspension for efficient GQDs production. While this method is physically straightforward, it is less efficient and not ideal for large-scale production due to its long processing times and low yield.<sup>63</sup> Traditional atmospheric pressure ultrasonic treatment often yields uneven graphene sheets, with variable size and shape.<sup>64</sup> However, high-pressure ultrasonic treatment can overcome these limitations by providing sufficient energy to disrupt the van der Waals forces between graphene layers more effectively.<sup>65</sup> This enhanced method accelerates reaction rates, increases yield, and shortens preparation time, showing promise for more efficient and scalable GQDs production.

Other top-down approaches, such as hydrothermal methods,<sup>66,67</sup> electrochemical oxidation with an external power source,<sup>68</sup> chemical vapor deposition (CVD),<sup>69</sup> pulsed laser ablation (PLA),<sup>70,71</sup> or their combinations,<sup>72</sup> offer additional avenues for GQD synthesis. These methods can enhance environmental friendliness, stability, and overall performance in producing high-quality GQDs.

### Down-Top Method

The down-top preparation method for GQDs involves the gradual assembly of carbon atoms or small molecules into graphene structures.<sup>73</sup> This technique leverages the conversion of small polycyclic aromatic hydrocarbons (PAHs) and related molecules into GQDs.<sup>74</sup> Typically, carbon source materials, which are small organic molecules, are carefully selected and subjected to specific heating conditions to produce carbon atoms or clusters. These carbon atoms or clusters are then deposited and crystallized in the presence of suitable catalysts through techniques such as CVD or alternative methods.<sup>75</sup>

During the deposition process, the morphology and size of the graphene structures can be finely controlled by adjusting parameters such as temperature, atmospheric conditions, and deposition duration. Additionally, surfactants or ligands are often incorporated during the preparation to regulate the morphology of the GQDs and enhance their stability. The final GQDs are obtained through a series of extraction, separation, and purification steps.<sup>76</sup>

The down-top method can be further categorized into four primary techniques based on the external energy supply and manufacturing characteristics: hydrothermal method, microwave-assisted hydrothermal method, soft-template method, and metal catalysis.<sup>74</sup> These techniques allow for precise control over the graphene structure, facilitating the tuning of optical, electrical, and chemical properties of the GQDs. However, this method has its limitations. Despite the environmentally friendly nature of molecular carbonization, it often results in products with lower purity.<sup>77</sup> Additionally, the down-top approach involves complex reaction steps and requires specific organic materials, making condition optimization challenging.<sup>78</sup> Electron beam irradiation, while capable of producing large quantities rapidly, is costly.<sup>79</sup> Therefore, the choice of preparation technique must be carefully considered based on the specific application requirements.

### Preparation of GNS

GNS can be prepared through various methods, one of which is the longitudinal unzipping of multi-walled carbon nanotubes (MWCNTs) using sulfuric and nitric acids. This method is favored for its minimal cytotoxicity<sup>80</sup> and allows for the oxidation and reduction of GNS. Potassium permanganate is used to oxidize GNS into GO nanosheets, while concentrated ammonium hydroxide (NH<sub>4</sub>OH) and N<sub>2</sub>H<sub>4</sub> are used to reduce GO to rGO nanosheets. Dimiev et al have detailed that GNS formation involves oxidative decompression of MWCNTs, which is likely driven by intercalation, oxidation, and subsequent peel-off.<sup>81</sup>



Guoxiu Wang et al refined the Hummers and Offeman method to synthesize GNS from natural graphite.<sup>82</sup> In their approach, graphite powder is reacted with concentrated nitric and sulfuric acids (in a 1:2 volume ratio), followed by the addition of  $\text{KClO}_3$  in an ice bath. The mixture is oxidized for 120 hours to produce GO. After washing the GO with deionized water to achieve a neutral pH, it is suspended in a mixture of ethanol and water and treated with ultrasonic waves for one hour, yielding a yellow-brown nanosheet suspension. The GO solution is then reduced to GNS by refluxing with hydroquinone for 20 hours. This method is advantageous due to its thorough oxidation and reduction processes and its emphasis on environmental sustainability.

Furthermore, Zhi Yang et al developed a shear-assisted supercritical  $\text{CO}_2$  exfoliation (SSCE) process in 2016.<sup>83</sup> This technique utilizes the shear stress exerted by supercritical  $\text{CO}_2$  fluid under high temperature and rotational speed to expand and delaminate graphite into GNS. This method offers a novel approach to graphene nanosheet preparation, leveraging the unique properties of supercritical  $\text{CO}_2$  for effective exfoliation. Characterization results reveal that 90% of the graphene produced via the SSCE method comprises sheets with fewer than 10 layers, with approximately 70% having 5 to 8 layers. This graphene exhibits exceptional electrical conductivity, reaching up to  $4.7 \times 10^6$  S/m. The SSCE method demonstrates superior GNS production efficiency compared to traditional methods involving the reduction of GO, offering a streamlined, rapid, and cost-effective approach for large-scale production of high-quality GNS.

## Rational Design of Graphene-Based Nanomaterials for Toxicity Reduction

Despite diverse synthesis methods for GO, rGO, GQDs and GNS enabling the modulation of hazardous by-products generation, surface chemistry and structure, their inherent toxicity remains a key barrier to tumor therapy. Unmodified graphene-based nanomaterials can induce physical membrane damage via nanoknife-like edges,<sup>84,85</sup> trigger oxidative stress through surface-bound reactive oxygen moieties (eg, epoxide groups),<sup>86</sup> and accumulate in reticuloendothelial organs due to size-dependent clearance limitations.<sup>87</sup> Such inherent toxicity poses a critical barrier to future clinical translation, necessitating rational design strategies to transform graphene-based nanomaterials into biocompatible PDT platforms.

To fully exploit the therapeutic potential of graphene-based nanomaterials in cancer treatment while minimizing toxicity, recent research progress has been centered around the engineering design of graphene interfaces guided by the structure-activity relationship. Researchers have systematically adjusted the surface chemistry, dimensionality, and composite structure of graphene. As a result, they have developed “stealth” graphene-based nanomaterials. These materials may enhance PDT efficacy while ensuring biosafety, reducing harm to healthy tissues and cells. The functionalization of graphene-based nanomaterials with organic chromophores mitigates toxicity by passivating reactive graphene interfaces and enhances therapy through precise optoelectronic tuning, further contributing to the improved performance of graphene-based nanomaterials in PDT.

Organic chromophores form dense  $\pi$ - $\pi$  stacked layers or covalent networks on graphene surfaces, effectively masking reactive edges and oxygen-containing groups.<sup>88</sup> For porphyrin-graphene covalent coupling, amide and diazo bond additions are common strategies. However, amide bond addition is limited by the scarcity of carboxyl groups on GO, while its oxygen-containing defects compromise graphene's intrinsic properties. In contrast, diazo bond coupling forms stable networks that may better shield reactive sites and preserve graphene's performance in ultralow-voltage photonic synaptic devices.<sup>89</sup> Meanwhile, ultrafast electron transfer from organic polymer nanoparticles or photoswitchable chromophores to GO reduces its oxidation potential, thereby suppressing ROS formation and mitigating oxidative toxicity. For instance, rapid electron transfer minimizes oxygen-induced oxidation, effectively lowering ROS generation.<sup>90</sup> Additionally, modulating the dipole moment of chromophores through isomerization regulates charge transfer with graphene,<sup>91</sup> further stabilizing its oxidation state and reinforcing toxicity shielding via chromophore-graphene interactions.

There are mainly two strategies for the functionalization synthesis of graphene-based nanomaterials and organic chromophores. In Strategy 1, the chromophore serves as the core element, functioning both as a PS and a toxicity-shielding layer. This inherent multifunctionality eliminates the need for additional functional modules, thereby simplifying synthesis. To support long-term therapeutic use, covalent bonding with graphene ensures structural stability and sustained performance. This is evidenced by rGO-porphyrin, where diazonium coupling improves solubility and non-linear optical responses.<sup>92</sup> The advantage of Strategy 1 lies in the direct coverage of graphene's reactive sites by chromophores, which mitigates oxidative stress and mechanical damage. Nevertheless, graphene-based nanocomposites

derived from Strategy 1 tend to possess limited functional versatility due to their single-component design. Moreover, the efficiency of covalent functionalization is limited by the availability of surface reactive sites on graphene, posing a challenge for GO-organic chromophore conjugates, particularly given the low density of carboxyl groups on GO.

In Strategy 2, the chromophore is integrated with other functional modules, such as targeting ligands, catalytic nanoparticles, and imaging probes, to enable multimodal therapy and diagnosis. This integration allows for a combination of PDT, targeted drug delivery, and catalytic therapy (eg, alleviating hypoxia). The synergistic actions of the different modules enhance therapeutic efficacy by overcoming the limitations of single-modality treatments. Strategy 2 often employs non-covalent interactions to accommodate high loading capacity and enable dynamic responsiveness. A representative example of Strategy 2 is the rGO quantum dot (rGOQD)/IR820/MnO<sub>2</sub> nanocomposite, in which the chromophore IR820 is combined with the catalytic module MnO<sub>2</sub>. MnO<sub>2</sub> catalyzes the decomposition of H<sub>2</sub>O<sub>2</sub> into O<sub>2</sub>.<sup>93</sup> This multimodal system enhances ROS generation under NIR light, improves PDT efficacy, and enables targeting of hypoxic or hard-to-reach tumors, aligning with the principles of multifunctional integration and synergistic enhancement. However, the multicomponent integration in Strategy 2 necessitates precise control over the stoichiometric ratios and spatial arrangement of each functional module. This increases the complexity of the nanoplatform design. These two representative strategies are illustrated in Figure 5, which provides a schematic overview of their respective design principles, functional components, and therapeutic mechanisms.

## Strategies in PDT for Tumor Treatment

### Development of Advanced Photosensitizers

PSs are pivotal to the success of PDT as they are responsible for transferring light energy to a reactant, catalyzing a chemical reaction while remaining unchanged chemically.<sup>94</sup> The representative of the first generation of PSs are hematoporphyrin derivatives (HPDs).<sup>95</sup> HPDs' ability to selectively target tumor cells and accumulate within them has been a cornerstone of its usage, though the exact mechanisms of its action are yet to be fully elucidated.<sup>96</sup> While HPDs exhibit preferential tumor uptake, their prolonged retention in normal tissues induces severe dark cytotoxicity and cutaneous phototoxicity, necessitating weeks of post-treatment light avoidance.<sup>97</sup> Moreover, the strong hydrophobicity<sup>98</sup> of HPDs limits their solubility in physiological environments, leading to aggregation and reduced bioavailability. This aggregation not only diminishes their photodynamic efficacy but also restricts their ability to diffuse effectively through the tumor extracellular matrix (ECM),<sup>99</sup> thereby impairing deep tissue penetration.

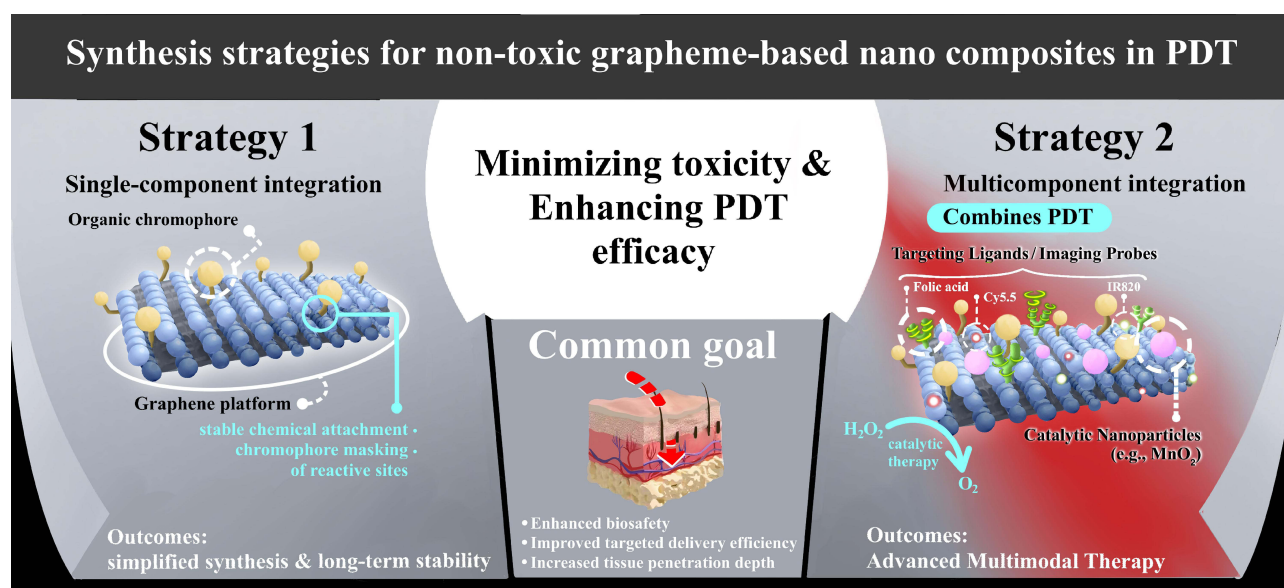


**Figure 5** Two functionalization strategies for producing non-toxic graphene-based nanocomposites to enhance PDT efficacy.

The quest for improvement led to the development of second-generation PSs, which include substances like 5-aminolevulinic acid (5-ALA), dihydroporphyrin, chlorophyll degradation derivatives, metal phthalocyanines, and benzoporphyrins.<sup>100</sup> The development of second-generation PSs was primarily driven by the need to address the shortcomings of their first-generation counterparts. These second-generation PSs offer several notable advantages, including longer absorption wavelengths, activation by near-infrared (NIR) light, greater penetration depth, higher singlet oxygen quantum yields, improved tissue selectivity, and a faster metabolism that helps reduce side effects.<sup>94</sup> Despite extended absorption into the NIR range, tissue penetration remains a significant limitation, as exemplified by 5-ALA, which penetrates only <2 mm into tissue when externally applied, restricting its ability to reach and eliminate affected lesions.<sup>101</sup> Concurrently, rapid renal clearance necessitates precise coordination between PS administration and light delivery, a challenge compounded by heterogeneous tumor vascularization.<sup>102</sup> Furthermore, another critical drawback of certain second-generation PSs, such as metal phthalocyanines, is their inherent tendency to self-aggregate. This aggregation significantly reduces  $^1\text{O}_2$  production, as their photochemical activity is primarily attributed to monomeric species.<sup>103</sup> Beyond diminishing photoactivity, aggregation also hinders cellular uptake and bioavailability, further limiting therapeutic efficacy.

These persistent challenges have spurred the development of third-generation PSs. This latest iteration is characterized by innovative modifications, such as the conjugation of PSs with specific molecular components like antibodies, carbohydrates, amino acids, or peptides, or their encapsulation in biocompatible carriers such as liposomes, micelles, and nanoparticles.<sup>104</sup> These enhancements are designed to mitigate off-target effects and optimize pharmacokinetic properties, thus increasing the accumulation of PSs at targeted sites.<sup>105</sup>

The rapid advancements in nanotechnology have played a pivotal role in this evolution, leading to the emergence of various nanomaterials that serve as either nano-PSs or carriers for PSs.<sup>94</sup> These third-generation PSs are engineered to rapidly metabolize, minimizing long-term presence in the body and reducing side effects. They exhibit a heightened selectivity for cancer cells, ensuring that they precisely target and destroy malignant cells while sparing healthy tissue. Enhanced hydrophilicity is also critical, improving systemic dispersion and enabling more effective drug distribution throughout the body.<sup>106</sup> Due to the limited water solubility of many PSs, employing nanomaterial-based carriers has become crucial for effective delivery to target cells, enhancing both targeting capabilities and overall therapeutic efficacy. These carrier platforms not only improve the biocompatibility and stability of PSs but also enhance their targeting ability, thus optimizing pharmacokinetic properties in vivo and increasing accumulation within tumor cells.

With ongoing innovations in nanotechnology, the potential to further refine and expand the design and application of third-generation PSs continues to grow. This advancement promises more precise and effective treatment options for various tumor types, representing a significant step forward in the field of PDT. Such progress may potentially revolutionize cancer treatment by providing increasingly sophisticated and effective therapeutic tools.

Graphene-based nanomaterials, including GO, rGO, and GQDs, introduce innovative solutions that enhance the performance of third-generation PSs. By precisely tailoring their structure and electronic properties, these materials significantly enhance the excitation efficiency of PSs and their ROS generation capabilities. Specifically, GO and rGO are noted for facilitating efficient energy transfer and dynamic electron interactions, as evidenced in recent studies.<sup>90,107</sup> Concurrently, GQDs offer tunable photoluminescence properties that are critical for boosting ROS generation.<sup>108</sup> Furthermore, GNS, characterized by their high surface area and excellent biocompatibility, improve the loading and targeted delivery of PSs.<sup>109</sup> These advancements effectively address critical limitations such as solubility and aggregation, thus opening new avenues for more precise and effective PDT.

## Enhancing Photodynamic Therapy Efficacy Through Optimized Light Source Selection

PDT critically hinges on the intricate interplay between light and tissue, a process that directly influences the activation of the PS. The nature of this interaction is primarily dictated by the light's inherent properties along with the absorption and scattering characteristics of the biological tissue.<sup>110,111</sup> Importantly, the optical penetration depth of the light within tissue is highly dependent on its wavelength, with depths ranging merely between 5–6 millimeters for wavelengths of 700–800 nm.<sup>112</sup> Given that PDT mandates localized light delivery, its application is predominantly confined to tumors that are either directly accessible to light or reachable through optical fibers. The limited light penetration depth further restricts PDT's therapeutic application, confining its use mainly to superficial cancers.<sup>113</sup>

During PDT, light excitation leads to the generation of either free radicals (Type I process) or  $^1\text{O}_2$ , (Type II process). These reactive species interact with surrounding oxygen, initiating cellular mechanisms that culminate in cell death. The generation of  $^1\text{O}_2$  is notably the most prevalent reaction pathway in PDT.<sup>114</sup> However, the penetration depth of the light - and thus the reach and effectiveness of PDT - is curtailed not only by the light's wavelength but also by scattering mechanisms and PS absorption. This combination of factors limits the broader applicability of PDT.<sup>115</sup> The penetration depth of light in tissue correlates with the effective attenuation coefficient, encompassing both absorption and scattering properties, and is influenced logarithmically by various PS characteristics including concentration, absorption coefficient, quantum yield, and other phenomena like saturation and photobleaching. Additionally, the light intensity and exposure duration are pivotal in determining the therapeutic outcome.<sup>116</sup>

The selection of an appropriate light source for PDT should be guided by the tumor's location, the required light dosage, and the properties of the chosen PS. Currently, clinical implementations of PDT utilize a spectrum of light sources. Laser sources such as the red argon (Ar) dye laser and the neodymium-doped yttrium aluminum garnet (Nd:YAG) laser provide precise light delivery. Alternatively, non-laser sources like traditional lights and LEDs (with red at 635 nm, green at 520 nm, and blue at 420 nm) offer a broader range of application.<sup>117–119</sup> Even natural daylight has been effectively harnessed in certain treatment protocols, showcasing the adaptability and broad potential of PDT in clinical settings.<sup>120</sup> This strategic choice of light sources underscores the necessity of integrating advanced optical science with therapeutic precision to enhance PDT's efficacy against diverse cancer types.

Laser sources are highly valued in PDT for their precision and efficiency. Among non-laser alternatives, LEDs stand out due to their affordability, safety, minimal risk of thermal damage, and the flexibility in array design configurations.<sup>121</sup> Despite these advantages, both laser and non-laser light sources face a significant challenge: their penetration depth is limited to a modest 1–6 mm.<sup>6</sup> This restriction greatly undermines their effectiveness in treating deeper-seated tumors. The primary obstacles to deeper light penetration are twofold. Firstly, endogenous chromophores such as hemoglobin, myoglobin, and cytochromes can absorb visible light, directly competing with the PS and thus diminishing the efficacy of the photodynamic process.<sup>122</sup> Secondly, the complex heterostructure of biological tissues can cause light to scatter, diffuse, and become disoriented, further impairing the therapeutic impact of PDT.<sup>123</sup>

Addressing the challenge of limited light penetration has become a pivotal focus in enhancing PDT efficacy. Recent advancements indicate that nanomaterial carrier platforms, especially those customized with specific functional substances, provide a promising avenue to optimize PS subcellular localization and overcome these limitations.<sup>124–126</sup> Notably, platforms constructed from graphene and graphene-based nanomaterials are being explored due to their exceptional optical properties, presenting a viable solution for enhancing PDT's reach.

A notable development in this arena is the innovative approach by Proshkina's research team at the Russian Academy of Sciences, as published in *Light: Science & Applications*.<sup>127</sup> They introduced a gene-encoded bioluminescence resonance energy transfer (BRET)-activated PDT using a synthesized pair of NanoLuc-miniSOG BRET. This pair combines NanoLuc luciferase with the phototoxic flavoprotein miniSOG, creating a system that effectively generates ROS upon the injection of the luciferase substrate-without the need for external light exposure. Their experiments demonstrated impressive outcomes, achieving up to 72% tumor growth inhibition in mice solely through the internal generation of light. Furthermore, through the HER2-specific lentiviral delivery of the NanoLuc-miniSOG gene, tumor inhibition in xenograft mice reached 67%. These findings underscore the potential of the gene-encoded NanoLuc-miniSOG pair as a powerful nanoplatform for PDT, showing substantial promise for the treatment of deep-seated lesions and expanding the therapeutic scope of photodynamic interventions.<sup>128</sup>

## Biological Mechanisms of PDT-Induced Tumor Control

PDT has emerged as a potent anti-tumor phototherapy strategy, with its clinical applications in oncology tracing back to 1978 at the Roswell Park Cancer Institute.<sup>12</sup> The process of PDT involves two critical stages: first, the administration of a photosensitizing agent, followed by the activation of this agent using non-thermal light at a specific wavelength.<sup>129</sup> This section delves into the mechanisms through which PDT exerts its anti-tumor effects, which can be broadly categorized into three distinct areas:



1. ROS: Photodynamic reactions produce ROS, which can aggressively target tumor cells, culminating in either apoptosis (programmed cell death) or necrosis.<sup>130</sup>
2. Vascular Disruption: PDT directly damages the vascular system of the tumor and adjacent healthy blood vessels, leading to a disruption in oxygen and nutrient supply. This results in ischemia and hypoxia within the tumor microenvironment (TME), as illustrated in Figure 6.
3. Immune Response Activation: PDT can trigger inflammatory responses and initiate anti-tumor immunity, ultimately contributing to tumor destruction.<sup>132–134</sup>

Resistance to apoptosis is a hallmark of cancer progression, where the regulation of key apoptotic signaling pathways significantly impacts the efficacy of PDT in inducing tumor cell death.<sup>135</sup> Apoptosis is a precisely regulated and extensively studied mode of cell death, playing a crucial role in cellular growth, anti-tumor defenses, and the maintenance of the intracellular environment. Under PDT, autophagy may serve as an initial rescue mechanism, where cells attempt to phagocytize and remove damaged proteins. Apoptosis is typically triggered when PDT-induced damage surpasses the cell's capacity to repair, leading to irreparable cellular injury.<sup>129</sup>

Caspases, the executioners of apoptosis, induce characteristic biochemical and morphological changes in dying cells.<sup>136</sup> These changes include the cleavage of nuclear lamins accompanied by chromatin condensation and nuclear shrinkage; fragmentation of DNA following the cleavage of the inhibitor of caspase-activated DNase (CAD); and the breakdown of cytoskeletal proteins, which facilitates the formation of apoptotic bodies.<sup>137</sup>

Two primary pathways activate apoptosis:

1. Intrinsic Apoptotic Pathway: Initiated when the PS binds to mitochondrial membranes under light exposure, resulting in the release of cytochrome C and other cysteine activators from the mitochondria into the cytoplasm. This cascade activates caspases 3, 6, 7, and 8, with caspase 8 particularly involved in cleaving the endoplasmic reticulum protein Bap 31, triggering apoptosis.<sup>104</sup>
2. Extrinsic Apoptotic Pathway: Triggered by the activation of death receptors such as DR3, TNF $\alpha$ R, Fas, and DR4 by their respective ligands. These ligands initiate signal transduction, oligomerizing the receptor and activating the caspase cascade. Ligands activates and initiates apoptosis by summoning the initiator Caspase-8.<sup>138</sup>

Furthermore, the Bcl-2 family of proteins, which are known to regulate mitochondrial apoptosis, play a pivotal role.<sup>139</sup> Photodamage to Bcl-2 proteins in human cell lines can significantly enhance the apoptotic process by reducing the activity of caspases 3 and 6, thus promoting cell death.<sup>140</sup> This dual-pathway activation underscores the complexity and efficacy of PDT in cancer treatment, offering multiple avenues for therapeutic intervention.

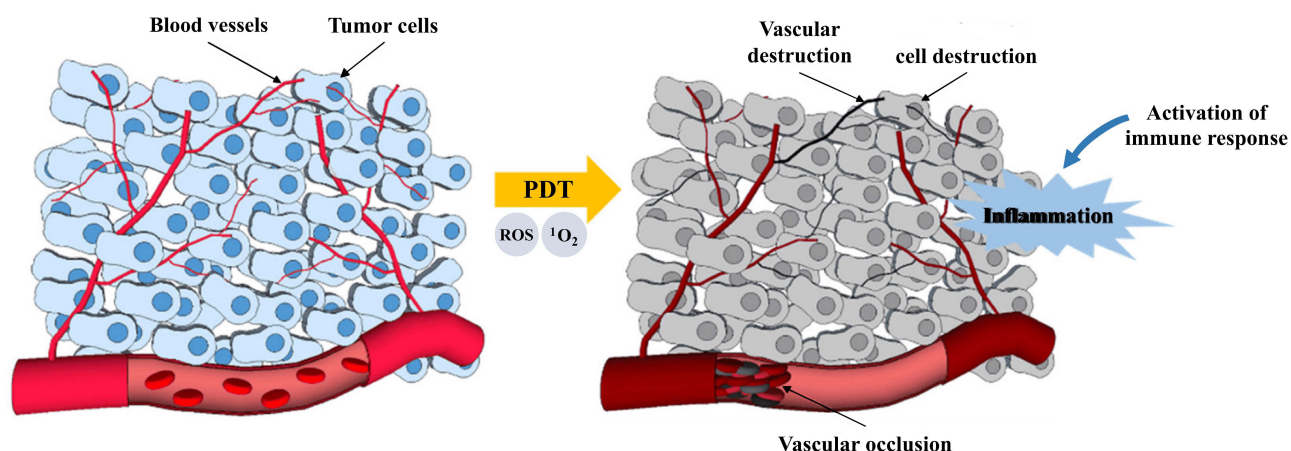


**Figure 6** Mechanism of PDT destruction of tumor. Reproduced from Correia JH, Rodrigues JA, Pimenta S, Dong T, Yang Z. Photodynamic Therapy Review: principles, Photosensitizers, Applications, and Future Directions. *Pharmaceutics*. 2021;13(9):1332. Under CC BY 4.0 <https://creativecommons.org/licenses/by/4.0/>.<sup>131</sup>



PDT involves the selective destruction of tumor cells through either Type I or Type II photochemical reactions. The PS absorbs photons and transitions to its first excited singlet state ( $S_1$ ).<sup>141</sup> In a Type I reaction, the PS, after absorbing light energy, loses an electron from the  $S_1$  state to form a radical cation ( $PS^+$ ).<sup>142</sup> This radical cation then reacts directly with surrounding  $O_2$ , producing ROS such as  $^1O_2$ , superoxide anions, and hydroxyl radicals. These ROS are highly oxidative and can damage cellular structures, kill bacteria, or inhibit the growth of abnormal cells. Type I reactions are advantageous because the PS has a lower oxidation potential, making it effective even in hypoxic environments where it can still produce  $^1O_2$ , which is more toxic than the products of Type II reactions.<sup>143</sup>

In Type II reactions, the PS relaxes rapidly to its first excited triplet state ( $T_1$ ) upon light absorption. From this state, the PS interacts with  $O_2$ , converting triplet oxygen ( $^3O_2$ ) to  $^1O_2$ , leading to tumor cell eradication.<sup>144</sup> The ROS generated in this process can interact with various cellular molecules, triggering a cascade of chemical reactions that result in cellular damage, apoptosis, or inhibition of abnormal cell growth. Figure 7 illustrates the reaction pathways of Type I and Type II photochemical reactions in PDT under PS activation.<sup>145</sup> The effectiveness of PDT is contingent upon adequate  $O_2$  supply, and its efficacy can be compromised in hypoxic tissues.<sup>146</sup> Currently, most researchers believe that the primary mechanism by which PSs damage tumor cells is via Type II reactions.<sup>132</sup>

PDT is predicated on the synergistic interaction of three primary components: the light source, molecular oxygen, and the PS. Together, these elements are crucial for the generation of highly cytotoxic ROS. The yield of ROS is a pivotal factor in determining the efficacy of PDT, as a higher ROS output correlates with enhanced apoptosis of malignant cells and, consequently, more effective tumor treatment. The performance of the PS is particularly significant as it influences

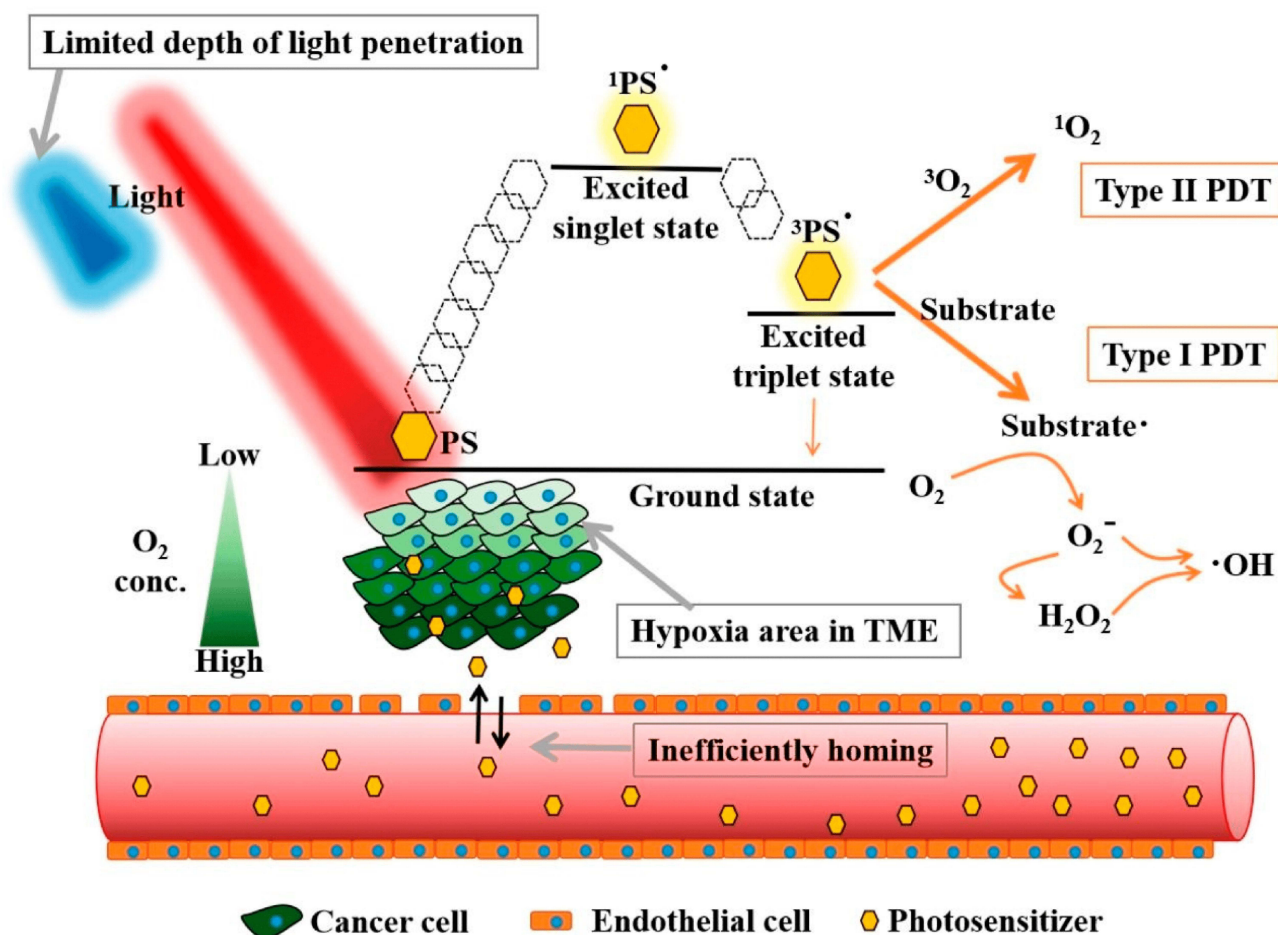


**Figure 7** Schematic diagram of photochemical reactions of Type I and Type II involved in PDT under the action of PS. Reproduced from Li W-P, Yen C-J, Wu B-S, Wong T-W. Recent Advances in Photodynamic Therapy for Deep-Seated Tumors with the Aid of Nanomedicine. *Biomedicines*. 2021;9(1):69. Under CC BY 4.0 <https://creativecommons.org/licenses/by/4.0/>.<sup>147</sup>

both the light source's effectiveness and oxygen utilization, ultimately affecting the precision of the tumor-targeting mechanism. PDT leverages the selective accumulation of the PS in pathological tissues, enabling the targeted destruction of these tissues while sparing surrounding healthy tissues. This selectivity and therapeutic efficacy position PDT as a preferable option compared to other oncological treatments.<sup>148,149</sup>

The chemical architecture of the PS is vital as it affects its photosensitivity, photostability, and subcellular localization, which in turn determines the sites within the cell where ROS are generated. For instance, PSs that accumulate in mitochondria can inflict direct damage to these organelles, triggering apoptosis. A unique advantage of PDT is its spatial control over treatment; light is precisely directed to the tumor, ensuring ROS generation is confined to the tumor site and immediate vicinity. This localized activation of the PS minimizes damage to adjacent healthy tissues. Moreover, by adjusting parameters such as light wavelength, intensity, and exposure duration, clinicians can finely tune PDT to maximize its impact on tumor cells while minimizing collateral damage.<sup>150</sup>

## Utilization of Graphene-Based Nanomaterials in Photodynamic Therapy

Graphene, a remarkable material consisting of a single layer of carbon atoms arranged in a two-dimensional honeycomb lattice, stands out for its exceptional properties. With its monolayer thickness of just 0.335 nm, graphene is one of the thinnest stable crystal structures known.<sup>151</sup> Unlike spherical nanoparticles, the ultrathin nature of graphene-based nanomaterials minimizes steric hindrance<sup>152</sup> and allows them to slip through the dense ECM network more efficiently.<sup>153</sup> This structural advantage significantly enhances their intratumoral penetration compared to bulkier three-dimensional nanoparticles. It boasts extraordinary electrical conductivity, an impressive specific surface area, notable mechanical strength and biocompatibility. Notably, graphene is one of the most thermally conductive materials known.<sup>154</sup> Its exceptional optical properties further enhance its biomedical applications. With a transmittance rate of up to 97.7% as the highest among two-dimensional materials, graphene allows deep tissue penetration of light in PDT, thereby improving PS excitation efficiency and enhancing therapeutic effects.<sup>155</sup> Moreover, its extremely low reflectivity, which is less than 0.1%, and minimal light absorption, at approximately 2.3%, result in reduced energy loss. This ensures efficient light utilization in PDT.<sup>156</sup>

The photophysical and photobiological performance of graphene-based nanocomposites in PDT is strongly governed by their electronic structures and excited-state behaviors. Ground-state electronic properties, such as bandgap and charge carrier dynamics, significantly influence light absorption and energy conversion. For example, due to GO's abundant oxygen-containing groups, exhibits a finite bandgap (about 4 eV),<sup>157</sup> enabling absorption in the visible region. In contrast, with rGO's partially restored  $sp^2$  carbon network, displays a narrower bandgap (<1 eV),<sup>158</sup> making it highly responsive to NIR irradiation. This bandgap modulation enables rGO to support plasmonic resonance under NIR light, thereby amplifying local electromagnetic fields and enhancing PS excitation. Charge carrier dynamics also play a crucial role. Surface defects in GQDs act as electron traps that extend exciton lifetimes, enhancing ROS generation.<sup>159</sup> Nitrogen-doped graphene quantum dots exhibit prolonged exciton lifetimes compared to undoped GQDs, leading to enhanced ROS generation.<sup>160</sup> This characteristic significantly improves the efficacy of PDT by increasing oxidative stress on target cells, thereby enhancing the therapeutic outcome.<sup>161</sup> In the excited state, graphene-based nanocomposites mediate diverse interactions that further influence PDT outcomes. Förster resonance energy transfer (FRET) can occur when GQDs act as energy acceptors,<sup>162</sup> quenching PS fluorescence while channeling energy to neighboring PS molecules. Additionally, under NIR excitation, plasmonic rGO can inject hot electrons directly into PSs such as IR780,<sup>163</sup> bypassing the conventional singlet-triplet transition and enabling Type I PDT pathways that are more tolerant to hypoxia. Moreover, the non-radiative decay pathways associated with graphene materials, particularly GO with high defect densities, convert a large fraction of absorbed light into thermal energy. A molecular dynamics study demonstrated that the thermal conductivity of GO decreases monotonically with increasing oxidation. When the oxidation level reached 10%, the thermal conductivity dropped by approximately 90%, suggesting that higher defect densities hinder phonon transport and enhance local heat retention, thereby facilitating more efficient photothermal conversion.<sup>164</sup> This localized hyperthermia not only enhances PS uptake through increased tumor membrane permeability<sup>165</sup> but also contributes directly to protein denaturation and tumor ablation, creating a synergistic effect with PDT.<sup>166</sup>

## Functional Role of GO in PDT

GO is produced by treating graphite with strong oxidizing agents, which introduces epoxy, hydroxyl, and carboxyl groups to the graphite surface. These oxygen-containing functional groups enhance GO's hydrophilicity relative to graphene, improving its solubility and dispersion in various solvents.<sup>167</sup> This high hydrophilicity and extensive surface area facilitate GO's interaction with water molecules in living organisms,<sup>168</sup> thereby improving its bioavailability and therapeutic efficacy in PDT for tumors. Furthermore, the reactive oxygen-containing groups on GO enable its chemical modification, promoting the development of GO-based nanomaterials.<sup>169</sup> However, GO's dispersibility in protein- or salt-rich environments, such as cell culture media and serum, can be low, which may lead to dose-dependent toxicity. Thus, GO typically requires modification through covalent or non-covalent conjugation before it can be effectively used as a nanocarrier in PDT.<sup>170</sup>

TME, GSH levels significantly mitigate the cytotoxic ROS produced through PDT and nanoenzyme catalysis. However, GO demonstrates promise in modulating oxidative stress within the TME due to its GSH-depletion and peroxidase-like activities.<sup>171</sup> These capabilities have spurred modifications of GO to enhance PDT efficacy. For example, Xianhe Sun et al explored the application of PEGylated nano-graphene oxide (NGO) incorporating aggregation-induced emission (AIE) nanoparticles as an innovative PDT agent. Despite the high potential of AIE nanoparticles in PDT, their stability and efficacy in physiological saline solutions remain suboptimal. To overcome this limitation, the team enhanced the stability of NGO in phosphate-buffered saline (PBS) through PEGylation and incorporated dual-functional AIE molecules, creating NGP-TPE-red nanoparticles. These nanoparticles, which comprise PEGylated NGO encapsulating tetraphenylethylene (TPE), not only exhibit red fluorescence under certain conditions but also effectively image blood vessels in mouse ears and UMUC3 cells. More importantly, NGP-TPE nanoparticles have shown significant tumor growth inhibition in both *in vitro* and *in vivo* models, demonstrating the stability and potential of AIE nanoparticle-encapsulated NGO in PDT.<sup>172</sup>

In a complementary approach, Feng Liu et al demonstrated that while unmodified GO alone does not generate  $^1\text{O}_2$ , its combination with gold nanoparticles (AuNPs) leads to significant  $^1\text{O}_2$  production, enhancing its utility in PDT. They developed a multifunctional nanocarrier (NGO-AuNPs-FA/methylene blue, MB) by loading AuNPs onto NGO, surface-modifying the complex with SH-PEG1000-FA via Au-S bonds, and electrostatically adsorbing MB as a PS. This configuration substantially augmented the antitumor effects *in vitro*, showcasing a strategy to exploit GO's surface properties for synergistic enhancement of PDT.<sup>173</sup>

Further enhancing targeted PDT, Peng Huang et al utilized folic acid-conjugated GO (FA-GO) to load PS chlorin e6 (Ce6). The Ce6 was efficiently loaded onto FA-GO through hydrophobic interactions and  $\pi$ - $\pi$  stacking, resulting in enhanced Ce6 accumulation within tumor cells and a potent photodynamic effect against GC cells MGC803. The folate-mediated targeting of this system takes advantage of the overexpression of folate receptors on many cancer cells,<sup>174</sup> improving targeting of tumor cells for more efficient Ce6 delivery than to normal cells. The FA-GO-Ce6 is internalized via a folate receptor-mediated pathway and releases Ce6 in the lysosomal environment, triggering a PDT effect upon irradiation with appropriate wavelength and dose. This nanocarrier system not only improves drug solubility and bioavailability but also enhances cytotoxicity against tumor cells while minimizing toxicity to normal tissues. Future research could focus on refining the size and modifying the surface properties of GO-based delivery systems to prevent fluorescence quenching and further boost PDT efficacy.<sup>175</sup>

Given GO's strong absorption in the NIR region,<sup>176</sup> it has been utilized for low-power NIR laser PTT. The combination of GO-based PDT with PTT presents promising new avenues for next-generation cancer therapies. A dual-mode treatment platform under single-wavelength laser irradiation represents a highly promising development direction with substantial potential for biomedical applications.<sup>177</sup> Poliraju Kalluru et al demonstrated that in GO-PEG-Folate, GO acts as a PS by directly absorbing light energy and facilitating the formation of  $^1\text{O}_2$ .<sup>178</sup> This approach eradicated B16-F0 melanoma tumors in mice using dual-mode nanomaterial-mediated PDT (NmPDT) and PTT (NmPTT) with an ultra-low NIR light dose ( $0.36 \text{ W/cm}^2$ ) at 980 nm *in vivo*, negating the need for additional PS.

Tian et al developed a method for loading PS Ce6 onto PEG-functionalized GO through supramolecular  $\pi$ - $\pi$  stacking.<sup>32</sup> The resulting GO-PEG-Ce6 complex exhibited excellent water solubility and substantially enhanced intracellular PS transport, thereby improving targeted destruction of tumor cells. The combination of PDT and PTT with this



complex markedly increased Ce6 delivery to tumor cells.<sup>179</sup> Figure 8 illustrated that after a 20-minute incubation of GO-PEG-Ce6 with tumor cells, followed by 5 minutes of 660 nm laser irradiation, effective tumor cell kill was achieved.<sup>83</sup> Further, a combined treatment with 20 minutes of 808 nm laser irradiation followed by 5 minutes of 660 nm laser exposure resulted in even greater tumor cell death, demonstrating the significant therapeutic enhancement from the PDT-PTT synergy.

These studies underscore the progress in enhancing PDT and combined therapies through functionalized GO, improving stability in aqueous solutions and PS accumulation in tumor cells. Xianhe Sun's PEG-NGO encapsulated AIE nanoparticles demonstrated significant tumor inhibition in both in vitro and in vivo PDT applications.<sup>172</sup> Feng Liu's NGO-AuNPs-FA/MB nanocarrier exhibited excellent performance in combined PDT and PTT therapy.<sup>173</sup> Peng Huang's FA-GO-Ce6 showed notable photodynamic effects in targeted PDT.<sup>175</sup> Poliraju Kalluru's<sup>178</sup> GO-PEG-FA nanomaterial enabled dual-mode PDT and PTT under ultra-low-dose NIR. Tian's research highlighted the potent tumor-killing efficiency of GO-PEG-Ce6 under the synergistic action of PDT and PTT.<sup>179</sup> These findings showcase the immense potential of GO-based nanomaterials in PDT. Continuous optimization of GO's structure and functional modifications is crucial, offering valuable insights for developing next-generation tumor treatment platforms.

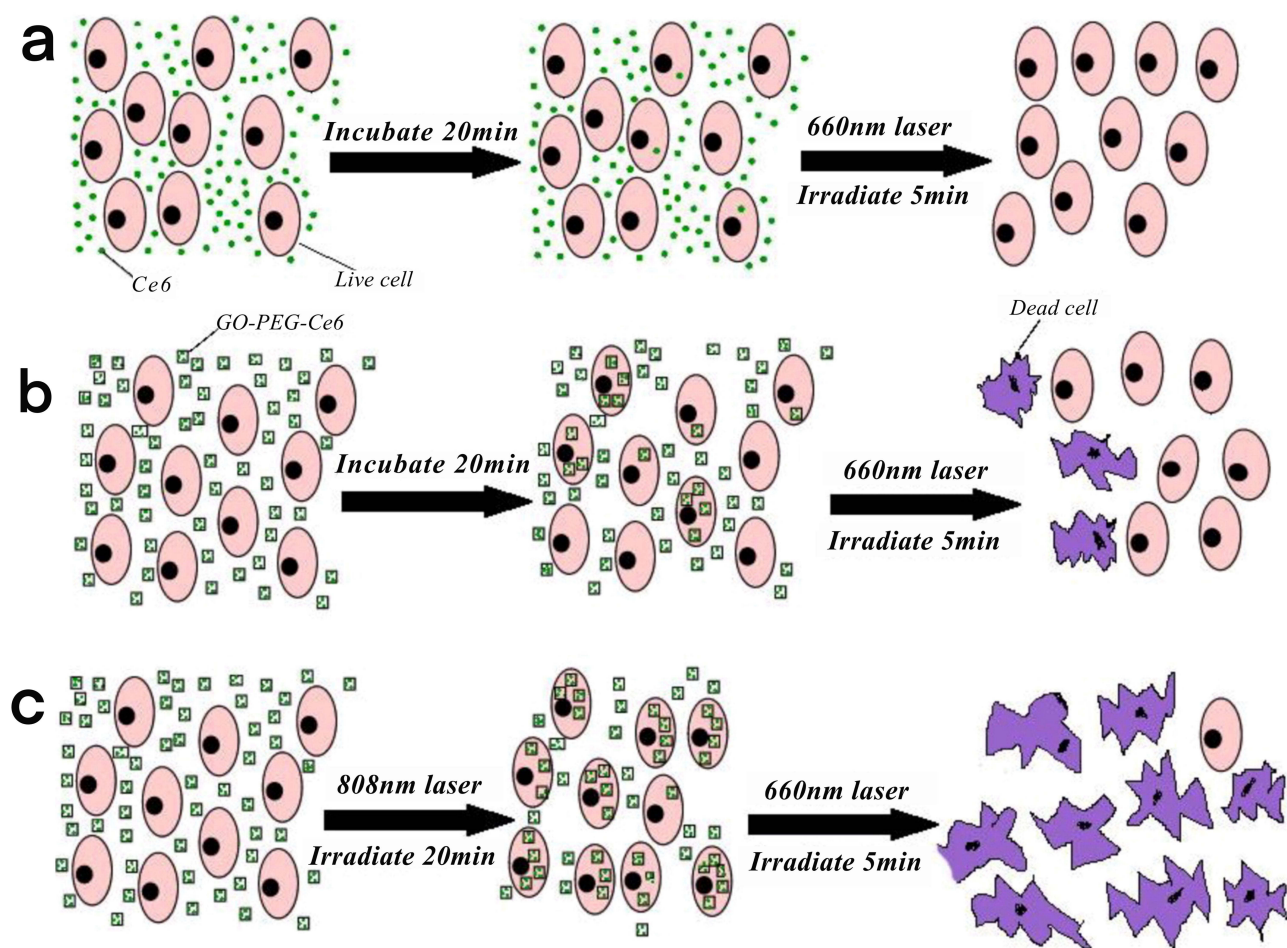


**Figure 8** Schemes of the experimental design in photothermally enhanced PDT. KB cells were incubated with free Ce6 (a) and GO-PEG-Ce6 (b) for 20 min in the dark and then irradiated by the 660 nm laser (50 mW/cm<sup>2</sup>, 5 min, 15 J/cm<sup>2</sup>) in control experiments. (c) To induce the photothermal effect, GO-PEG-Ce6 incubated cells were exposed to the 808 nm laser (0.3 W/cm<sup>2</sup>, 20 min, 360 J/cm<sup>2</sup>) first before PDT. Reproduced from Li Y, Dong H, Li Y, Shi D. Graphene-based nanovehicles for photodynamic medical therapy. *Int J Nanomed*. 2015;10:2451–2459.<sup>179</sup>

## Functional Role of rGO in PDT

In recent years, rGO has emerged as a significant component in the field of PDT, primarily due to its enhanced electrical conductivity and functional versatility following the reduction of GO. The reduced oxygen content and improved conductivity of rGO make it a favorable candidate for PDT applications.

One notable advancement is the modification of rGO with polyvinylpyrrolidone (PVP),<sup>180</sup> as reported by researchers who covalently attached an integrin-specific peptide (ACDCRGDCFCG, RGD4C) onto the PVP backbone via hydrogen bonding. This modification allows for the effective loading of the aromatic PS Ce6 into the rGO-PVP-RGD system through hydrophobic interactions and  $\pi$ - $\pi$  stacking. This approach markedly enhances the accumulation of Ce6 in tumor cells compared to the use of Ce6 alone, thereby significantly improving PDT efficacy.

Further research highlights the utility of rGO's specific surface area and its non-covalent interactions with porphyrins and drugs to enhance drug solubility in aqueous environments. For example, Ma et al developed an rGO-based nanocarrier platform that utilizes rGO's high surface area to improve the water solubility of THPPEG and various drugs.<sup>181</sup> As shown in Figure 9, this platform not only leverages the synergistic effects of PTT, PDT, and chemotherapy but also utilizes rGO as an efficient carrier for PS and drug delivery, thereby greatly enhancing antitumor efficacy.

In a related study, Kandasamy Vinothini and team engineered a versatile rGO-based system for combined chemotherapy and PDT.<sup>182</sup> This system involved functionalizing the rGO surface with magnetic nanoparticles and camptothecin (CPT), while cross-linking the PS 4-hydroxycoumarin (4-HC) with an allylamine linker. The CPT-loaded MrGO-AA-g-4-HC nanocarrier demonstrated pH-sensitive drug release and exhibited higher cytotoxicity against MCF-7 breast tumor cells compared to normal cells. Laser irradiation at 365 nm further amplified ROS production from 4-HC, promoting apoptosis in cancer cells. In vivo experiments confirmed the system's superior antitumor efficiency through the synergistic effects of chemotherapy and PDT, underscoring its potential for effective tumor treatment.

Wei-Jane Chiu et al demonstrated that FeOxH-rGO could generate ROS via the Fenton reaction and exhibit high photothermal conversion under NIR irradiation.<sup>183</sup> This combination of PDT and PTT proved effective in eradicating

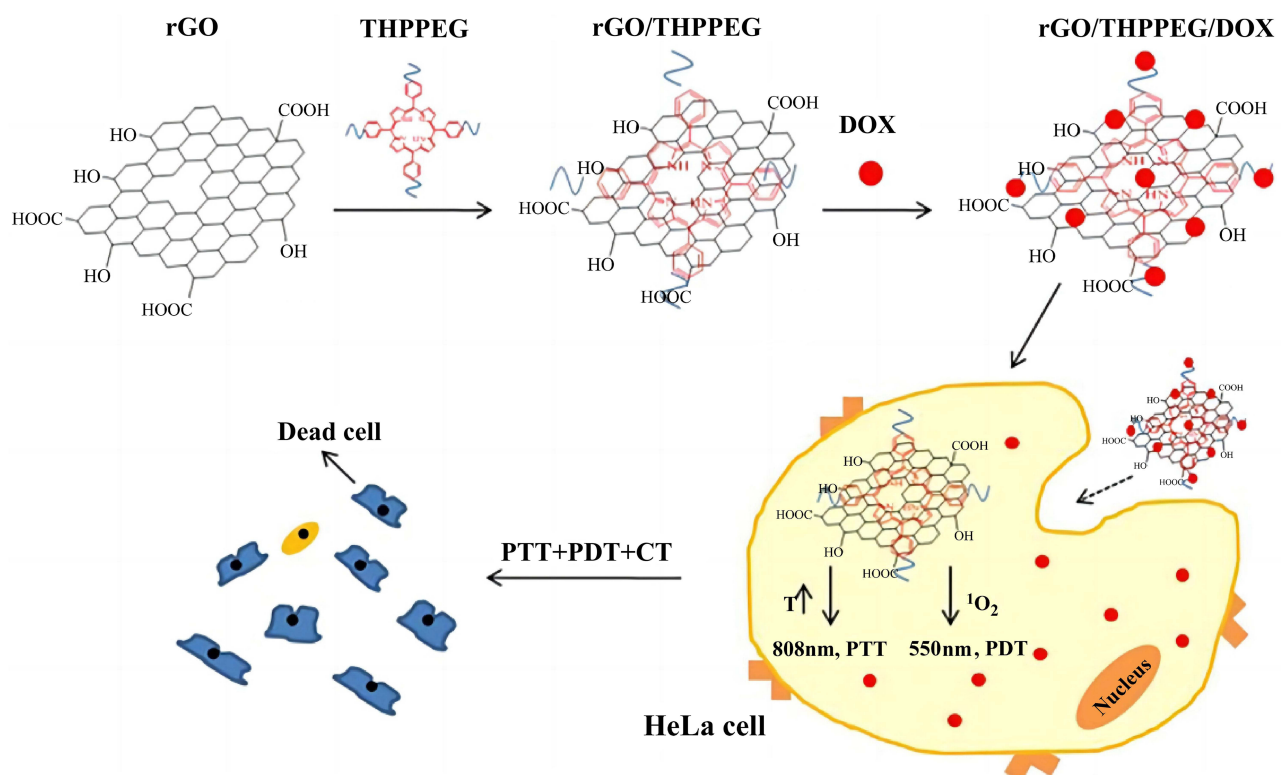


**Figure 9** Synthesis of rGO/THPPEG/DOX and its combined effect on PTT/PDT/CT. Reprinted from Ma W, Yang H, Hu Y, Chen L. Fabrication of PEGylated porphyrin/reduced graphene oxide/doxorubicin nanoplateform for tumour combination therapy. *Poly Int.* 2021;70(9):1413–1420. © 2021 Society of Industrial Chemistry.<sup>181</sup>



tumor cells with minimal recurrence or acute side effects, highlighting its potential clinical value. Similarly, Wenjing Jiang et al introduced a novel tumor-targeting nanoplatfrom using dopamine-rGO (rGO-PDA),<sup>184</sup> which was further coated with mesoporous silica and hyaluronic acid. This design enhanced photothermal conversion and allowed for controllable drug release under NIR irradiation. The platform efficiently delivered Ce6 to CD-44 over-expressing tumor cells, resulting in significantly improved singlet oxygen production and PDT efficiency. By integrating NIR-induced photothermal conversion with controlled Ce6 release, this nanoplatfrom effectively destroyed tumor cells, demonstrating robust potential for multimodal tumor therapy and targeted treatments.

Lastly, Smita et al reported on rGO modified with protoporphyrin IX (PPIX).<sup>185</sup> When exposed to a 635 nm laser, the rGO-PPIX system significantly increased ROS production in HeLa cells compared to HADF cells. This result indicated that the PDT system effectively eradicates tumor cells through Caspase-3 activation, further validating its potential in PDT applications. However, traditional PDT is constrained by factors such as low bioavailability, limited absorption bands, and inadequate tissue oxygenation. Kapri et al addressed these issues by developing a composite of MoS<sub>2</sub> nanosheets, approximately 5 nm thick, combined with nitrogen-doped reduced rGO.<sup>186</sup> This composite was further enhanced with PEG modification and MnO<sub>2</sub> surface decoration, significantly improving biocompatibility and colloidal stability. MnO<sub>2</sub> reacts with endogenous H<sub>2</sub>O<sub>2</sub> in cancer cells to alleviate hypoxia by increasing intracellular O<sub>2</sub> levels. Under NIR irradiation, this composite markedly increased HeLa cell apoptosis and PDT efficacy, showcasing its substantial potential for therapeutic applications.

Despite advancements, some PDT nanomaterials, like Fe-soc-MOF nanoparticles,<sup>187,188</sup> face therapeutic limitations and potential immunogenicity.<sup>189</sup> Bruna L. Melo et al tackled these challenges by functionalizing dopamine-rGO with sulfobetaine methacrylate brushes to create IR780/SB/DOPA-rGO.<sup>190</sup> This innovative NIR-responsive nanocomposite, designed for combination PDT-PTT, demonstrated excellent biocompatibility in vitro (cell viability >78%) and reduced breast cancer cell survival to 21% at low doses without causing immunogenicity.<sup>191</sup> This approach provides fresh insights into overcoming the limitations of existing nanomaterials in tumor treatment.

## Functional Role of GQDs in PDT

GQDs are emerging as exceptional carriers for PS delivery due to their small size, expansive surface area, and remarkable biocompatibility. GQDs excel in PDT by generating <sup>1</sup>O<sub>2</sub> through polymorphism sensitization (MSS: S<sub>1</sub>→T, T→S<sub>0</sub>). Their outstanding photoluminescence, strong water dispersibility, and high biocompatibility facilitate efficient cellular uptake and enhanced <sup>1</sup>O<sub>2</sub> production. Under 470 nm blue light irradiation, GQDs produce ROS that induce oxidative stress and lead to the death of U251 cells.<sup>192</sup> Compared to traditional PS PPIX, GQDs generate <sup>1</sup>O<sub>2</sub> at twice the rate, demonstrating superior PDT performance in both in vitro and in vivo studies.<sup>193</sup>

GQDs, consisting of monolayers of graphene ranging from several to dozens of nanometers, exhibit distinct optical penetration properties due to quantum confinement and edge effects.<sup>194</sup> These properties enable GQDs to perform effectively in PDT. ROS generation by GQDs is facilitated by all oxygen-containing functional groups, with ketone groups inducing the highest levels of ROS.<sup>195</sup> Notably, GQDs do not induce cytotoxicity in dark conditions.<sup>196</sup>

Markovi et al<sup>192</sup> reported that electrochemically prepared GQDs generate ROS, including <sup>1</sup>O<sub>2</sub>, under blue light (470 nm, 1 W), leading to apoptosis and autophagy in U251 glioma cells. As shown in Figure 10, Ge J et al found that GQDs, as PS, exhibit superior photostability compared to PPIX and CdTe quantum dots.<sup>193</sup> Unlike conventional PS that require UV/Vis irradiation, which limits light penetration depth and therapeutic efficacy, GQDs operate across a broader range of wavelengths, thus enhancing PDT effectiveness.<sup>197</sup>

Du et al developed innovative redox-responsive, photoactive GQD nanocomposites by integrating Ce6 onto GQDs through disulfide bonds, with Pluronic F127 used as a stabilizer.<sup>198</sup> Upon reaching tumor tissues, glutathione (GSH) within the cells cleaves the disulfide bonds, releasing Ce6 and reactivating its phototoxicity. Despite fluorescence quenching and mild phototoxicity under illumination, the nanocomposites effectively restore the PS's activity in the presence of reducing agents. Both in vitro and in vivo studies demonstrated that this redox-responsive GQD nanocomposite significantly inhibits HeLa cell growth.

J. Anjusha et al prepared an up-conversion nanocomposite using amino acid-functionalized GQDs (af-GQDs /UCNPs).<sup>199</sup> They employed the DCFH-DA reagent as a fluorescent probe to detect intracellular ROS. After entering

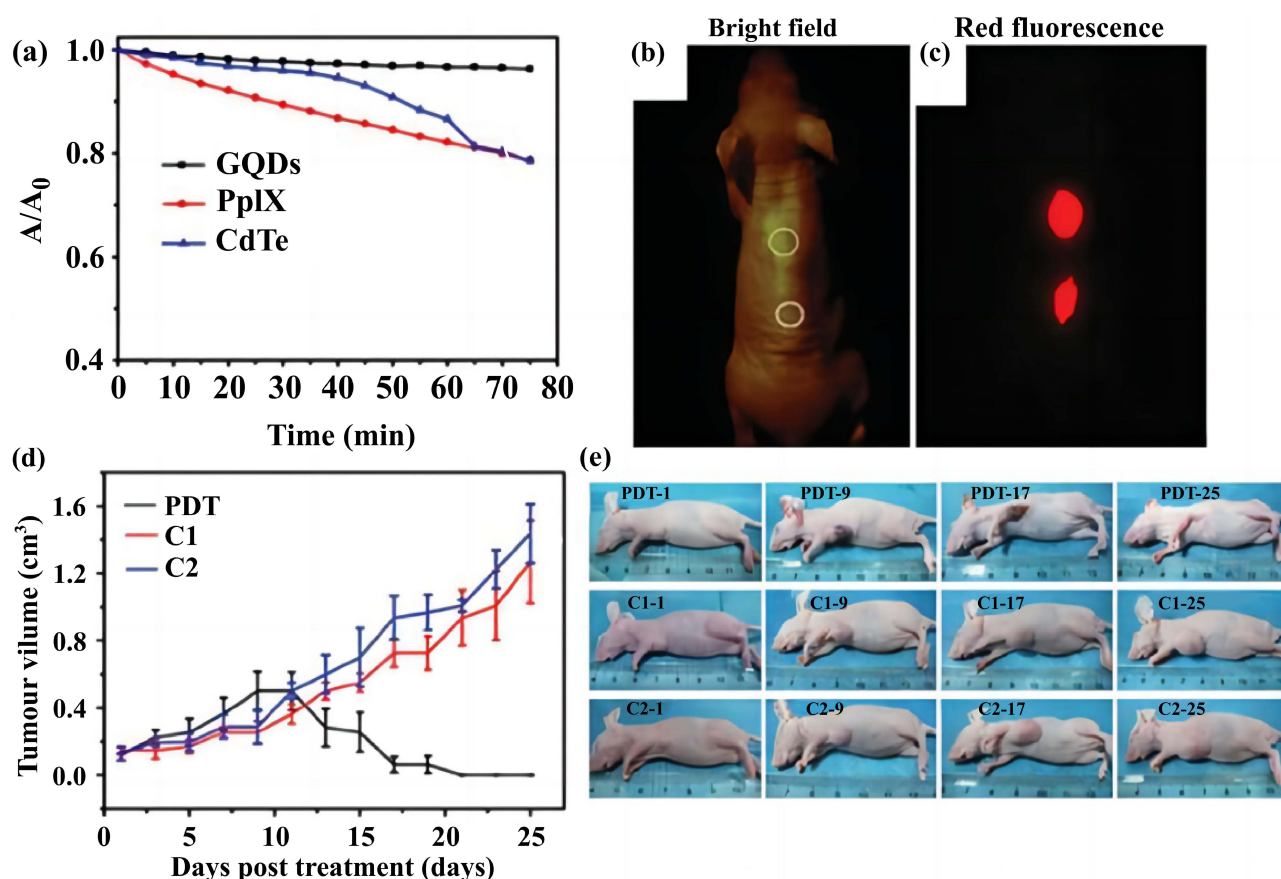


**Figure 10** (a) Comparison of photostability for GQDs, PpIX, and CdTe, indicated by the absorbance ratio at 470 nm over time post-irradiation with a 500 W xenon lamp. (b) Bright-field image and (c) red-fluorescence image of a mouse following subcutaneous GQD injection. (d) Tumor volume measurements over time for three treatment groups ( $n = 5$  per group), with significant differences ( $P < 0.05$ ). PDT: GQD with irradiation, C1: GQD alone, C2: light irradiation alone. (e) Photographs of mice post various treatments, with the numbers indicating days after the initial treatment. Reproduced with permission from Ge J, Lan M, Zhou B, et al. A graphene quantum dot photodynamic therapy agent with high singlet oxygen generation. *Nat Commun.* 2014;5(1):4596..<sup>193</sup>

the cells, DCFH-DA was hydrolyzed to the non-fluorescent compound DCFH, which was subsequently oxidized by ROS into the highly fluorescent dichlorofluorescein (DCF). In the referenced study, HeLa cervical cancer cells were co-incubated with af-GQDs/UCNPs, stained with Hoechst, and then irradiated with a 532 nm laser ( $0.1 \text{ W/cm}^2$ , 1 min) to induce ROS generation. The resulting DCF emitted strong green fluorescence at 535 nm when excited at 485 nm. Fluorescence imaging was performed using 485 nm excitation, and cells treated with the nanocomposite exhibited intense green fluorescence post-irradiation, confirming elevated ROS production and demonstrating the nanocomposite's potential for light-activated PDT against tumor cells,<sup>200</sup> as shown in Figure 11.

Curcumin, a biocompatible polyphenol derived from turmeric, has demonstrated enhanced water solubility when loaded onto GQDs, as shown by Sana Mushtaq et al.<sup>201</sup> This combination significantly improves the PS activity of curcumin, leading to an increased production of ROS and enhanced anticancer efficacy under visible light. Curcumin-loaded GQDs further exhibit potent inhibitory effects on human colon cancer cells during PDT.<sup>202</sup> To address the challenges of repeated PDT cycles, acidity-activated GQD nanotransformers (GQD NTs) have been developed to optimize PS delivery and mitigate side effects.<sup>203</sup> These nanotransformers facilitate improved tumor targeting, retention, and penetration through acidity-triggered deformation. Moreover, laser-induced mild hyperthermia enhances PS uptake, enabling efficient repeated PDT with significantly reduced PS doses and minimized toxicity, thereby demonstrating their potential to improve PDT efficacy.

In another significant development, Banendu Sunder Dash et al introduced a rGOQD/IR820/ $\text{MnO}_2$  nanocomposite that generates enhanced ROS production under NIR light.<sup>93</sup> The  $\text{MnO}_2$  component of this nanocomposite plays a critical

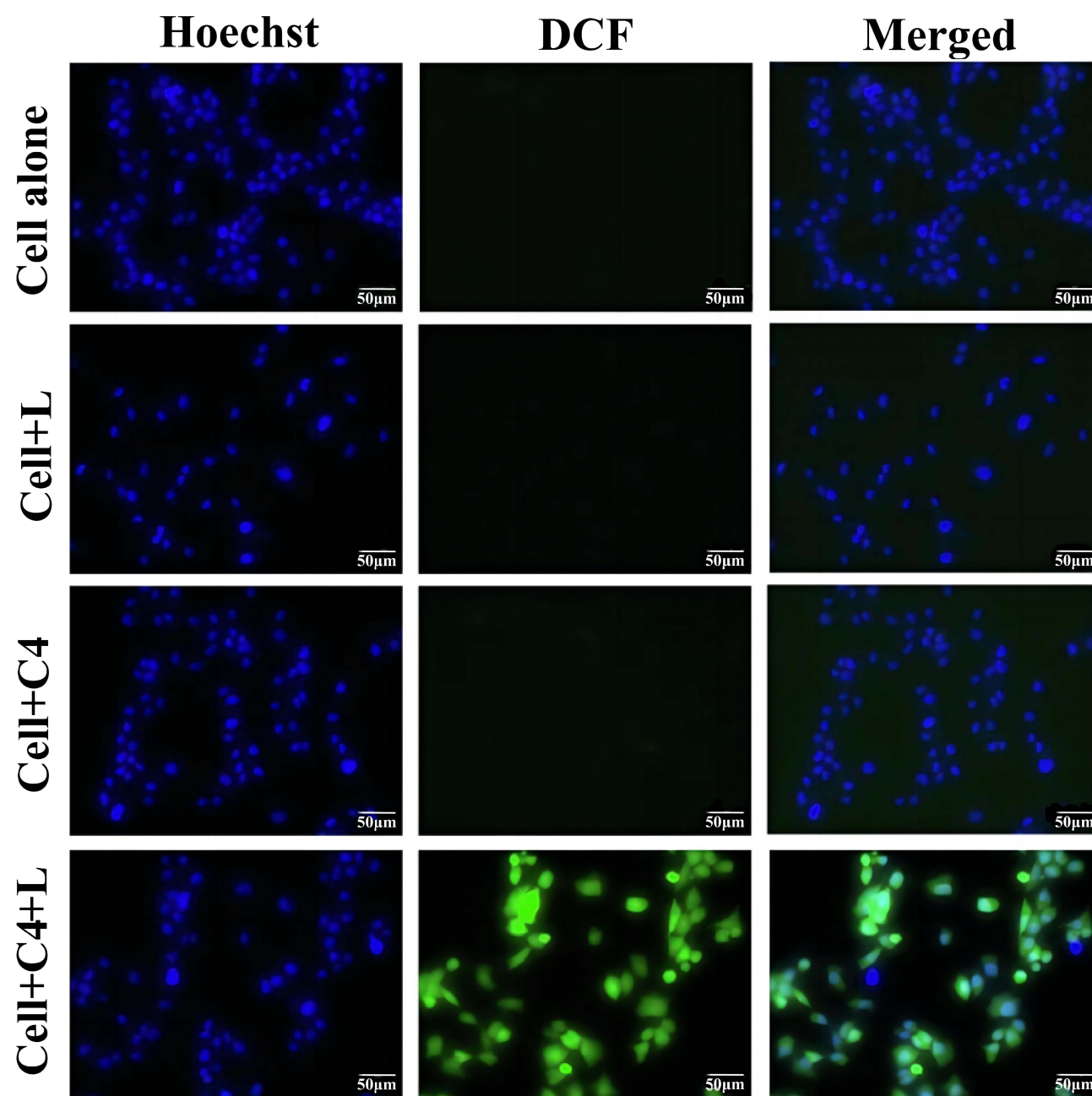


**Figure 11** Imaging analysis of in vitro PDT on HeLa cells with and without 532 nm laser using DCFDA fluorescent probe (L and C4 represent light and af-GQDs/UCNPs, respectively). Reprinted from Anjusha AJ, Thirunavukkarasu S, Resmi AN, Dhanapandian S, Krishnakumar N, Krishnakumar N. Multifunctional amino functionalized graphene quantum dots wrapped upconversion nanoparticles for photodynamic therapy and X-ray CT imaging. *Inorg Chem Commun.* 2023;149:110428. with permission from Elsevier.<sup>200</sup>

role in alleviating tumor hypoxia by catalyzing the conversion of  $\text{H}_2\text{O}_2$  into oxygen, thereby improving oxygen levels and promoting ROS generation. This enhancement substantially increases the effectiveness of PDT by facilitating tumor apoptosis. Furthermore, the ability of this nanocomposite to cross the blood-brain barrier holds promise for targeting challenging brain tumors, such as glioblastoma. Collectively, these advancements improve PDT by ensuring increased oxygen availability and selective nanoparticle accumulation at difficult-to-reach tumor sites.

In the context of combining PDT with immunotherapy, polyethylene glycol-functionalized GQD (GQD-PEG) has demonstrated remarkable synergistic effects.<sup>204</sup> In an oral squamous cell carcinoma model, laser-activated GQD-PEG achieved approximately 70% tumor inhibition by inducing apoptosis and producing  $^1\text{O}_2$ , with selective tumor targeting confirmed. Under irradiation, GQDs not only enhanced immune responses by boosting  $\text{CD}^{8+}$  T cell activity but also

promoted the release of pro-inflammatory cytokines. In the absence of irradiation, GQDs modulated dendritic cells through autophagy, thereby suppressing inflammation. This dual mechanism highlights the potential of GQD-PEG in synergistic cancer therapies.

Building on these advances, a plasmonic nanohybrid consisting of thiolated chitosan-coated gold nanostars (AuNS-TCS) and riboflavin-conjugated N,S-doped GQD (Rf-N,S-GQD) has been developed to overcome the limitations of conventional dual-therapy strategies that rely on a single low-power laser.<sup>178</sup> This integrated system combines two therapeutic modalities, targeted photodynamic therapy (TP-PDT) and PTT, achieving enhanced stability, improved  $^1\text{O}_2$  generation, and superior antitumor efficacy in both 2D and 3D tumor models. These findings underscore the potential of such advanced nanohybrids for clinical cancer therapy, offering a promising route toward more efficient, multifunctional therapeutic platforms.

GQDs have shown immense potential in PDT through various functional modifications and composite developments. Their size-dependent penetration, particularly sub-10 nm GQDs, enables deep tumor infiltration, enhancing treatment efficacy.<sup>205</sup> GQDs are effective in generating ROS to induce tumor cell death while maintaining photoreactivity under specific conditions without causing cytotoxicity. As research progresses, GQDs are anticipated to emerge as a next-generation material for PDT, offering novel approaches and methodologies for tumor treatment.

## Functional Role of GNS in PDT

In recent years, GNS have gained attention as a promising material for tumor treatment via PDT. GNS are characterized by their high surface area-to-volume ratio, which provides substantial drug-loading capacity for the efficient delivery of PS to targeted tumor cells. Furthermore, GNS exhibit excellent photothermal conversion efficiency under NIR irradiation, which enhances ROS production—critical for inducing cytotoxic effects on cancer cells. Targeted ligand-functionalized GNS can specifically recognize and bind to tumor cells, thereby improving the accumulation of PS within the TME.

For instance, Gang Liu et al developed an effective liquid-phase exfoliation method to prepare GNS-Ce6 with a high loading ratio of Ce6.<sup>206</sup> This composite demonstrated a remarkable enhancement in PDT efficacy, with improvements ranging from 7 to 75 times compared to previously reported nanomaterial-Ce6 composites. Additionally, Kaviyarasu et al highlighted that zinc oxide nanocrystal-modified GO nanosheets (GONS) can be utilized for high-performance photocatalytic applications.<sup>207</sup> Miao et al further demonstrated that PEG-functionalized GONS, when used as co-delivery carriers for anticancer agents and PS, significantly increased tumor cell targeting.<sup>208</sup> Functionalized GONS enhance drug uptake by tumor cells while promoting greater drug accumulation and aggregation within tumor tissues.

Dilpreet Singh et al have highlighted the innovative integration of graphene-peptide nanosheets, which combine graphene's remarkable mechanical strength with peptide functionalities.<sup>209</sup> These peptides are either covalently or non-covalently attached to the graphene surface, allowing for the precise customization of short-chain amino acids tailored to specific applications. When exposed to targeted wavelengths of light for PDT, these graphene-peptide nanosheets exhibit exceptional light absorption properties. They function as PSs, efficiently concentrating light on tumor cells within a short duration. This leads to a significant production of ROS in the tumor cells, initiating apoptosis and providing a targeted approach to tumor therapy.<sup>210</sup>

However, the TME is often characterized by severe hypoxia, which poses a challenge to effective treatment. Tumors frequently adapt by overexpressing antioxidants such as GSH, leading to drug resistance and diminishing therapeutic efficacy. To address this issue, Peng Liu et al have introduced a novel multifunctional nanoplatform incorporating manganese dioxide-doped GONS.<sup>211</sup> This platform is designed for the co-delivery of Cisplatin (CisPt) and Ce6. As depicted in Figure 12, the approach involves alleviating tumor hypoxia through self-oxygenation mechanisms and reducing intracellular GSH levels.<sup>211</sup> This modulation of the TME enhances the combined effects of PDT and chemotherapy, significantly improving tumor treatment outcomes.

In another development, Weihong Guo et al created GONS functionalized with PEG and oxidized sodium alginate (OSA), and loaded with paclitaxel (PTX).<sup>212</sup> This strategy was aimed at overcoming paclitaxel resistance in gastric cancer (GC). The GO-PEG-OSA nanosheets demonstrated high stability and excellent biocompatibility. They improve drug solubility, enhance bioavailability, and increase cytotoxicity against cancer cells while minimizing side effects. Upon NIR irradiation, these nanosheets exhibit significant photothermal effects, ROS generation, and accelerated PTX



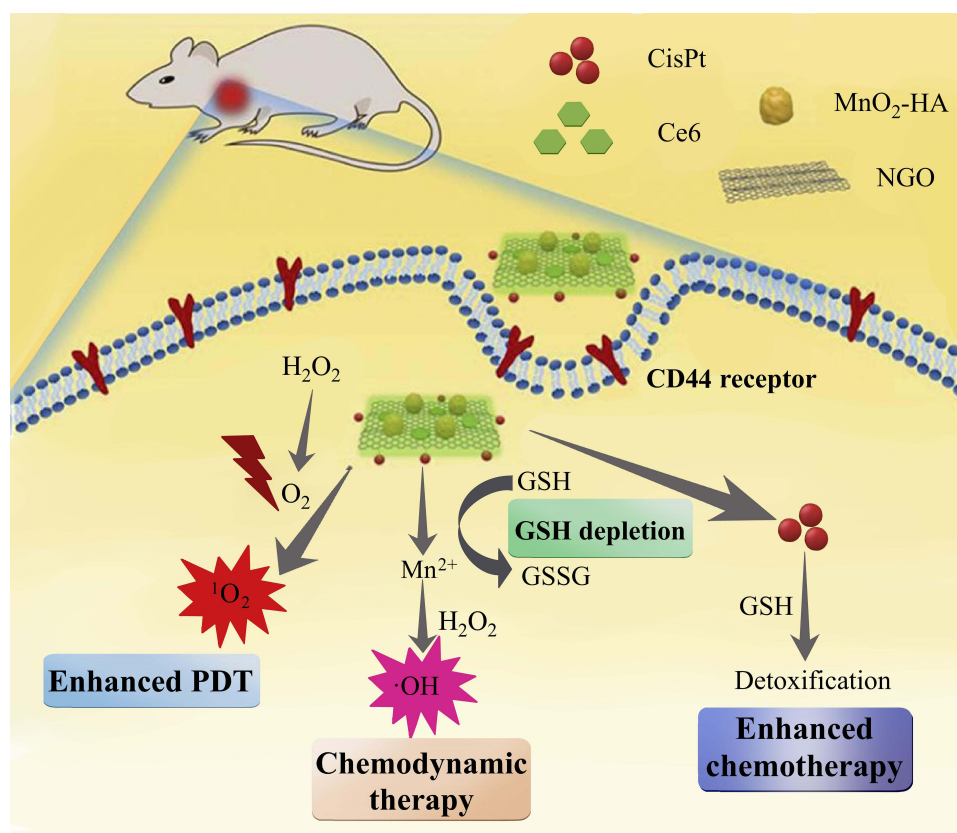


**Figure 12** GO/CisPt/Ce6@MH enhanced chemical-photodynamic synergistic therapy flow. Reproduced from Liu P, Xie X, Liu M, Hu S, Ding J, Zhou W. A smart MnO<sub>2</sub>-doped graphene oxide nanosheet for enhanced chemo-photodynamic combinatorial therapy via simultaneous oxygenation and glutathione depletion. *Acta Pharmaceutica Sinica B*. 2021;11(3):823–834. Under CC BY 4.0 <https://creativecommons.org/licenses/by/4.0/>.<sup>211</sup>

release due to heat. This combination of PDT, mild PTT, and chemotherapy markedly enhances drug sensitivity in drug-resistant GC cells, providing a synergistic therapeutic effect. This multifaceted approach represents a promising strategy for addressing drug-resistant gastric cancer.

Reza Hosseinzadeh et al investigated the interaction between MB as a PS and GONS in aqueous solutions for PDT applications.<sup>213</sup> Their research demonstrated that the GO-MB nanosheets, formed through electrostatic and  $\pi$ - $\pi$  stacking interactions, exhibited effective cytotoxicity against MDA-MB-231 breast cancer cells under red LED light, reducing cell viability by up to 20%. The study underscored that the GO/MB ratio significantly affects the PDT efficacy of the nanocomposite, with higher proportions of GO enhancing dimerization and catalytic efficiency. This finding underscores the potential of GO-based nanocomposites to markedly improve tumor cell eradication in PDT therapies.

Huaxiang Lu et al demonstrated a sophisticated approach utilizing rGO nanosheets (rGONS) combined with MnO<sub>2</sub> nanoparticles to enhance both PDT and chemotherapy.<sup>214</sup> The study involved loading doxorubicin (DOX), a chemotherapeutic agent, and MB onto the GO via strong physical interactions, which were subsequently released rapidly at elevated temperatures in the form of rGONS@MnO<sub>2</sub>/MB/DOX. The MnO<sub>2</sub> nanoparticles played a crucial role by catalyzing the conversion of tumor-internal H<sub>2</sub>O<sub>2</sub> into O<sub>2</sub>, facilitating the PDT process. In an in vivo carotid body tumor model, localized injection of rGONS@MnO<sub>2</sub>/MB/DOX followed by 808 nm NIR laser irradiation led to a significant reduction in tumor cell numbers and tumor volume, with no observable side effects. This innovative strategy presents a promising avenue for the integrated treatment of carotid body tumors. Additionally, the use of graphene nanosheets and their functional modifications enhances drug delivery efficiency and targeting accuracy. Multifunctional modifications and synergistic treatment approaches effectively tackle the challenges posed by the TME and drug resistance, offering valuable insights and laying a foundation for advancing PDT-based tumor therapies.

The advantages and disadvantages of graphene-based nanomaterials in PDT for tumor treatment are summarized in Table 1.



**Table 1** Advantages and Disadvantages of Graphene-Based Nanomaterials in PDT for Tumors Treatment

Name	Advantages	Disadvantages
GO	<ol style="list-style-type: none"> <li>1. Rich in oxygen-containing groups (eg, carboxyl, hydroxyl), allowing tunable solubility and biocompatibility<sup>167</sup></li> <li>2. Enhances PS drug-loading capacity and targeting through chemical modifications<sup>169</sup></li> <li>3. Enables multimodal therapy (PDT+PTT) in conjunction with NIR light<sup>178</sup></li> <li>4. High reactivity in biological environments improves therapeutic efficacy<sup>168</sup></li> </ol>	<ol style="list-style-type: none"> <li>1. Poor dispersibility in high-protein or high-salt environments<sup>170</sup></li> <li>2. Dose-dependent toxicity may limit applications<sup>170</sup></li> <li>3. Unmodified GO cannot independently generate <math>^1\text{O}_2</math><sup>173</sup></li> </ol>
rGO	<ol style="list-style-type: none"> <li>1. The reduced oxygen content of rGO restores its <math>\text{sp}^2</math>-hybridized carbon network, enhancing electron delocalization and thereby improving its electronic conductivity<sup>180,215</sup></li> <li>2. Non-covalent interactions (eg <math>\pi</math>-<math>\pi</math> stacking, hydrophobic forces) enable high loading capacity and protect payloads from premature leakage, facilitating controlled release and improved tumor-targeting efficiency<sup>181</sup></li> <li>3. The extended <math>\pi</math>-conjugated domains and large surface area of rGO improve energy transfer between the PS and incident light, thereby enhancing ROS generation<sup>183</sup></li> <li>4. Combined with <math>\text{MnO}_2</math> to alleviate tumor hypoxia<sup>186</sup></li> </ol>	<ol style="list-style-type: none"> <li>1. Unmodified rGO may have insufficient stability in complex biological environments<sup>182</sup></li> <li>2. PDT efficacy limited by tumor hypoxia and low bioavailability<sup>186</sup></li> </ol>
GQDs	<ol style="list-style-type: none"> <li>1. Unique quantum size and edge effects provide tunable fluorescence intensity and wavelength<sup>194</sup></li> <li>2. Efficient <math>^1\text{O}_2</math> production under blue light without dark toxicity<sup>196</sup></li> <li>3. High biocompatibility and dispersibility, allowing for functional modifications<sup>193</sup></li> <li>4. Superior photodynamic stability compared to traditional PS (eg PPIX)<sup>193</sup></li> </ol>	<ol style="list-style-type: none"> <li>1. Light absorption efficiency limited by surface chemistry and photon energy<sup>192</sup></li> <li>2. PDT efficiency restricted by light source wavelength and depth<sup>199</sup></li> </ol>
GNS	<ol style="list-style-type: none"> <li>1. High surface-to-volume ratio offers superior PS loading capacity<sup>207</sup> - Excellent photodynamic and ROS generation efficiency under NIR<sup>208</sup></li> <li>2. Multifunctional modifications (eg, PEG, <math>\text{MnO}_2</math>) regulate the TME for enhanced therapy<sup>211</sup></li> <li>3. Strong mechanical properties and biological stability<sup>210</sup></li> </ol>	<ol style="list-style-type: none"> <li>1. TME hypoxia and overexpression of antioxidants (eg, GSH) may hinder efficacy<sup>211</sup></li> <li>2. High drug-loading capacity may reduce controlled drug release<sup>212</sup></li> </ol>

To systematically summarize the targeting and penetration optimization strategies of graphene-based nanomaterials in PDT, this review compiles representative cases from the literature and categorizes them based on their optimization mechanisms. These strategies include receptor-mediated targeting, size-dependent penetration, optical synergy, and hypoxia modulation. Table 2 provides a clear overview of how these approaches enhance the therapeutic efficacy of graphene-based nanomaterials in PDT, further supporting the preceding discussion on their advantages and limitations.

Sometimes, these four strategies are not mutually exclusive. Instead, they often work in concert to enhance the targeting precision and tissue penetration of graphene-based nanomaterials in PDT. This interplay underscores the

**Table 2** Representative Cases for Targeting and Penetration Optimization Strategies of Graphene-Based Nanomaterials in PDT

Optimization Strategy	Graphene-Based Nanomaterial	Brief Mechanism Summary	Reference(s)
Receptor-mediated targeting	NGO-AuNPs-FA/MB, FA-GO-Ce6	Folate ligand enhances selective PS delivery to tumor cells.	[173, 175]
	rGO-PVP-RGD system	RGD modification promotes integrin-mediated uptake, boosting PS internalization.	[180]
	GQD-PEG, PEG-functionalized GONS	PEG modification improves systemic circulation and enhances tumor accumulation.	[204, 208]

(Continued)

**Table 2** (Continued).

Optimization Strategy	Graphene-Based Nanomaterial	Brief Mechanism Summary	Reference(s)
Size-dependent penetration	GQDs as PS	Superior photostability and broader wavelength absorption improve light penetration and PDT efficacy.	[193, 197]
	Electrochemically prepared GQDs	Small size facilitates tumor penetration while generating ROS under blue light, inducing apoptosis and autophagy in glioma cells.	[192]
Optical synergy	Combination of PDT, mild PTT, and chemotherapy	GO-PEG-OSA nanosheets enhance drug solubility and bioavailability while enabling ROS generation, photothermal effects, and heat-triggered PTX release under NIR, achieving PDT-PTT-chemo synergy to overcome drug resistance in gastric cancer.	[212]
	PDT-PTT	IR780/SB/DOPA-rGO enables NIR-triggered PDT-PTT synergy, reducing breast cancer cell survival to 21% at low doses without causing immunogenicity	[190, 191]
Hypoxia modulation	rGONS@MnO <sub>2</sub> /MB/DOX	rGONS serves as a structural scaffold, facilitating MnO <sub>2</sub> dispersion and stability while enhancing drug loading. MnO <sub>2</sub> reacts with excess H <sub>2</sub> O <sub>2</sub> in tumors, generating O <sub>2</sub> to relieve hypoxia and improve PDT efficacy.	[214]
	rGOQD/IR820/MnO <sub>2</sub>	rGOQD ensures MnO <sub>2</sub> stability and controlled release. IR820 enables NIR-triggered PTT for synergistic therapy.	[93]

multifaceted nature of nanomaterial-based PDT optimization. This review examines the current research perspectives in the field of PDT, with a specific focus on the applications of graphene-based nanomaterials to enhance PDT efficacy. Key challenges in the TME, such as hypoxia, will be discussed, along with strategies to address these issues, including O<sub>2</sub> delivery systems and the integration of multimodal therapies. By exploring these strategies, the review aims to highlight innovative approaches that can advance the development of graphene-based PDT platforms.

## Challenges and Prospect

Graphene-based nanomaterials hold significant promise in advancing PDT for tumor treatment due to their versatile properties. These materials can serve as platforms for loading PSs and drugs or function as PSs themselves, potentially enhancing the efficacy of PDT. Their unique attributes enable several strategies to improve tumor-targeted PS delivery and treatment outcomes.

One of the primary advantages of graphene-based nanomaterials is their ability to encapsulate PSs optimally, thereby protecting them from premature deactivation or leakage due to plasma interactions. This encapsulation also enhances the uptake of PSs within tumor tissues and cells, facilitating more precise and effective treatment. Moreover, the high transmittance of graphene-based materials allows for deeper light penetration, overcoming the inherent limitations of light sources in PDT and improving PS excitation efficiency.

Recent studies highlight the potential of graphene-based nanoplateforms for integrating PDT with other therapeutic modalities, leveraging the synergistic effects of combined treatments. This multimodal approach can lead to more comprehensive and effective tumor eradication strategies. However, there are notable challenges that need to be addressed.

A critical issue in PDT is O<sub>2</sub> transport to tumor cells. TMEs are often hypoxic due to uncontrolled cell proliferation and abnormal blood vessel formation. This hypoxia complicates PDT, as the process itself can deplete O<sub>2</sub> levels, further exacerbating hypoxic conditions and reducing therapeutic efficacy. Under such conditions, the generation of ROS is limited, which can restrict the depth of PDT penetration, affect the uniform distribution of PSs within tumors, and impair targeting precision. Additionally, hypoxic conditions can prompt tumor cells to enter dormancy or activate antioxidant mechanisms, further diminishing the effectiveness of PDT.

Graphene-based nanomaterials, with their high surface area, offer a promising solution to these challenges. They can be engineered to incorporate molecules or nanoparticles capable of delivering and releasing O<sub>2</sub> directly to the tumor site. Furthermore, these materials can embed catalysts that generate O<sub>2</sub> from endogenous substances such as H<sub>2</sub>O<sub>2</sub>, enhancing their therapeutic potential. However, this design requires precise control over the timing and location of O<sub>2</sub> release to synchronize with PS activation and ROS generation. Optimizing the release rates is crucial, as either excessively rapid or slow release can undermine treatment effectiveness. Additionally, catalysts must be specifically activated within the TME to avoid damaging normal tissues, and interactions between PSs and O<sub>2</sub> carriers need to be finely tuned to prevent interference and maximize synergistic effects.

In summary, while graphene-based nanomaterials offer significant potential for improving PDT outcomes, addressing these challenges requires further research. Advances in material design and understanding of tumor biology will be essential in overcoming these obstacles and enhancing the overall efficacy of PDT in cancer treatment. To facilitate clinical translation, future efforts should focus on optimizing surface functionalization to enhance biocompatibility and minimize immunogenicity. Development of stimuli-responsive and ligand-directed delivery systems may further improve tumor-specific targeting. In addition, integrating photothermal or immunomodulatory functions can potentiate synergistic therapeutic effects. Rigorous in vivo evaluations of metabolism and long-term safety remain essential to ensure clinical applicability. These efforts will be pivotal in bridging the gap between laboratory research and clinical application, paving the way for the next generation of PDT strategies based on graphene-based nanomaterials.

## Author Contributions

All authors made a significant contribution to the work reported, whether that is in the conception, study design, execution, acquisition of data, analysis and interpretation, or in all these areas; took part in drafting, revising or critically reviewing the article; gave final approval of the version to be published; have agreed on the journal to which the article has been submitted; and agree to be accountable for all aspects of the work.

## Funding

This work was supported by the National Natural Science Foundation of China [grant number 82173486], and the Key Research Program of the Tianjin Municipal Education Commission [Grant Number: 2023ZD009].

## Disclosure

The authors declare that they have no known competing financial interests or personal relationships that could have appeared to influence the work reported in this paper.

## References

1. Ganesh K, Massagué J. Targeting metastatic cancer. *Nat Med*. 2021;27(1):34–44. doi:10.1038/s41591-020-01195-4
2. Siegel RL, Kratzer TB, Giaquinto AN, Sung H, Jemal A. Cancer statistics, 2025. *Ca a Cancer J Clinicians*. 2025;75(1):10–45. doi:10.3322/caac.21871
3. Rugbjerg K, Mellekjaer L, Boice JD, Køber L, Ewertz M, Olsen JH. Cardiovascular disease in survivors of adolescent and young adult cancer: a Danish cohort study, 1943–2009. *J Natl Cancer Inst*. 2014;106(6):dju110. doi:10.1093/jnci/dju110
4. Peer D, Karp JM, Hong S, Farokhzad OC, Margalit R, Langer R. Nanocarriers as an emerging platform for cancer therapy. *Nat Nanotechnol*. 2007;2(12):751–760. doi:10.1038/nnano.2007.387
5. Kwon N, Weng H, Rajora M, Zheng G. Activatable Photosensitizers: from Fundamental Principles to Advanced Designs. *Angew Chem Int Ed*. 2025;64(15):e202423348. doi:10.1002/anie.202423348
6. Zhou Z, Song J, Nie L, Chen X. Reactive oxygen species generating systems meeting challenges of photodynamic cancer therapy. *Chem Soc Rev*. 2016;45(23):6597–6626. doi:10.1039/C6CS00271D
7. Yang S, Baeg E, Kim K. Neurodiagnostic and neurotherapeutic potential of graphene nanomaterials. *Biosens Bioelectron*. 2024;247:115906. doi:10.1016/j.bios.2023.115906
8. Patil S, Rajkuberan C, Sagadevan S. Recent biomedical advancements in graphene oxide and future perspectives. *J Drug Delivery Sci Technol*. 2023;86:104737. doi:10.1016/j.jddst.2023.104737
9. Iannazzo D, Celesti C, Espro C. Recent Advances on Graphene Quantum Dots as Multifunctional Nanoplatforms for Cancer Treatment. *Biotechnol J*. 2021;16(2):e1900422. doi:10.1002/biot.201900422
10. Iannazzo D, Celesti C, Giofrè SV, Ettari R, Bitto A. Theranostic Applications of 2D Graphene-Based Materials for Solid Tumors Treatment. *Nanomaterials*. 2023;13(16):2380. doi:10.3390/nano13162380
11. Tiwari SK, Sahoo S, Wang N, Huczko A. Graphene research and their outputs: status and prospect. *J Sci*. 2020;5:10–29.

12. Dougherty TJ, Kaufman JE, Goldfarb A, Weishaupt KR, Boyle D, Mittleman A. Photoradiation therapy for the treatment of malignant tumors. *Cancer Res.* **1978**;38(8):2628–2635.
13. Qu Y, He F, Yu CG, et al. Advances on graphene-based nanomaterials for biomedical applications. *Mater Sci Eng C Mater Biol Appl.* **2018**;90:764–780. doi:10.1016/j.msec.2018.05.018
14. Kim YJ, Hong IY, Shim J, An JC. Preparation and characterization of black liquor-derived activated carbon by self-chemical activation. *Carbon Lett.* **2020**;30:115–121.
15. Yao L, Chen A, Li L, Liu Y. Preparation, properties, applications and outlook of graphene-based materials in biomedical field: a comprehensive review. *J Biomater Sci-Polym Ed.* **2023**;34(8):1121–1156. doi:10.1080/09205063.2022.2155781
16. Razaq A, Bibi F, Zheng X, Papadakis R, Jafri SHM, Li H. Review on Graphene-, Graphene Oxide-, Reduced Graphene Oxide-Based Flexible Composites: from Fabrication to Applications. *Materials.* **2022**;15(3):1012. doi:10.3390/ma15031012
17. Brodie BC. On the atomic weight of graphite. *Philos Trans R Soc Lond.* **1859**;149:249–259.
18. London R. *Philosophical Transactions of the Royal Society of London.* W. Bowyer and J. Nichols; **1864**.
19. Hummers WS Jr, Offeman RE. Preparation of graphitic oxide. *J Am Chem Soc.* **1958**;80(6):1339. doi:10.1021/ja01539a017
20. Jr WSH, Offeman RE. Preparation of Graphitic Oxide. *J Am Chem Soc.* **1958**;80:1.
21. Shamaila S, Sajjad AKL, Iqbal A. Modifications in development of graphene oxide synthetic routes. *Chem Eng J.* **2016**;294:458–477. doi:10.1016/j.cej.2016.02.109
22. Kotai L, Gács I, Sajó IE, Sharma PK, Banerji KK. Beliefs and Facts in Permanganate Chemistry-An Overview on the Synthesis and the Reactivity of Simple and Complex Permanganates. *ChemInform.* **2011**;42(13). doi:10.1002/chin.201113233
23. Kovtyukhova NI, Ollivier PJ, Martin BR, et al. Layer-by-layer assembly of ultrathin composite films from micron-sized graphite oxide sheets and polycations. *Chem Mater.* **1999**;11(3):771–778. doi:10.1021/cm981085u
24. Zaaba N, Foo K, Hashim U, Tan S, Liu -W-W, Voon C. Synthesis of graphene oxide using modified hummers method: solvent influence. *Procedia Eng.* **2017**;184:469–477. doi:10.1016/j.proeng.2017.04.118
25. Chen X, Qu Z, Liu Z, Ren G. Mechanism of oxidization of graphite to graphene oxide by the hummers method. *ACS omega.* **2022**;7(27):23503–23510. doi:10.1021/acsomega.2c01963
26. Marciano DC, Kosynkin DV, Berlin JM, et al. Improved Synthesis of Graphene Oxide. *ACS Nano.* **2010**;4(8):4806–4814. doi:10.1021/nn1006368
27. Dimiev AM, Tour JM. Mechanism of Graphene Oxide Formation. *ACS Nano.* **2014**;8(3):3060–3068. doi:10.1021/nn500606a
28. Jiříčková A, Jankovský O, Sofer Z, Sedmudubský D. Synthesis and Applications of Graphene Oxide. *Materials.* **2022**;15(3):920. doi:10.3390/ma15030920
29. Liu J, Chen S, Liu Y, Zhao B. Progress in preparation, characterization, surface functional modification of graphene oxide: a review. *J Saudi Chem Soc.* **2022**;26(6):101560. doi:10.1016/j.jscs.2022.101560
30. Habte AT, Ayele DW. Synthesis and characterization of reduced graphene oxide (rGO) started from graphene oxide (GO) using the tour method with different parameters. *Adv Mater Sci Eng.* **2019**;2019:5058163. doi:10.1155/2019/5058163
31. Kotsyubynsky VO, Boychuk VM, Budzulyak IM, et al. Graphene oxide synthesis using modified Tour method. *Advm Natural Sci Nanosci Nanotechnol.* **2021**;12(3):035006. doi:10.1088/2043-6262/ac204f
32. Khan ZU, Kausar A, Ullah H, Badshah A, Khan WU. A review of graphene oxide, graphene buckypaper, and polymer/graphene composites: properties and fabrication techniques. *J Plast Film Sheeting.* **2016**;32(4):336–379. doi:10.1177/8756087915614612
33. Alam N, Sharma N, Kumar L. Synthesis of Graphene Oxide (GO) by Modified Hummers Method and Its Thermal Reduction to Obtain Reduced Graphene Oxide (rGO) \* Open Access. *Graphene.* **2017**;6(01):1–18. doi:10.4236/graphene.2017.61001
34. Tarcan R, Todor-Boer O, Petrovai I, Leordean C, Astilean S, Botiz I. Reduced graphene oxide today. *J Mater Chem C.* **2020**;8(4):1198–1224. doi:10.1039/C9TC04916A
35. Stankovich S, Dikin D, Piner R, et al. Synthesis of Graphene-Based Nanosheets via Chemical Reduction of Exfoliated Graphite Oxide. *Carbon.* **2007**;45(7):1558–1565. doi:10.1016/j.carbon.2007.02.034
36. Yang H, Hanyu G. Chemical synthesis of reduced graphene oxide: a review. *Minerals Mineral Mater.* **2023**;2:8.
37. Abdolhosseinzadeh S, Asgharzadeh H, Seop Kim H. Fast and fully-scalable synthesis of reduced graphene oxide. *Sci Rep.* **2015**;5(1):10160. doi:10.1038/srep10160
38. Fan ZJ, Kai W, Yan J, et al. Facile Synthesis of Graphene Nanosheets via Fe Reduction of Exfoliated Graphite Oxide. *ACS Nano.* **2011**;5(1):191–198. doi:10.1021/nn102339t
39. Fan Z, Wang K, Wei T, Yan J, Song L, Shao B. An environmentally friendly and efficient route for the reduction of graphene oxide by aluminum powder. *Carbon.* **2010**;48(5):1686–1689. doi:10.1016/j.carbon.2009.12.063
40. Yang S, Yue W, Huang D, Chen C, Lin H, Yang X. A facile green strategy for rapid reduction of graphene oxide by metallic zinc. *RSC Adv.* **2012**;2(23):8827–8832. doi:10.1039/c2ra20746j
41. Fan X, Peng W, Li Y, et al. Deoxygenation of Exfoliated Graphite Oxide under Alkaline Conditions: a Green Route to Graphene Preparation. *Adv Mater.* **2008**;20(23):4490–4493. doi:10.1002/adma.200801306
42. Lei Y, Tang Z, Liao R, Guo B. Hydrolysable tannin as environmentally friendly reducer and stabilizer for graphene oxide. *Green Chem.* **2011**;13(7):1655–1658. doi:10.1039/c1gc15081b
43. Dreyer D, Murali S, Zhu Y, Ruoff R, Bielawski C. Reduction of graphite oxide using alcohols. *J Mater Chem.* **2011**;21(10):3443–3447. doi:10.1039/C0JM02704A
44. Wang C, Chen Y, Zhuo K, Wang J. Simultaneous reduction and surface functionalization of graphene oxide via an ionic liquid for electrochemical sensors. *Chem Commun.* **2013**;49(32):3336–3338. doi:10.1039/c3cc40507a
45. Khanra P, Kuila T, Kim NH, Bae S, D-s Y, Lee J. Simultaneous bio-Functionalization and Reduction of Graphene Oxide by Baker's Yeast. *Chem Eng J.* **2012**;183:526–533. doi:10.1016/j.cej.2011.12.075
46. Bo Z, Shuai X, Mao S, Yang H, Qian J, Cen K. Green preparation of reduced graphene oxide for sensing and energy storage applications. *Sci Rep.* **2014**;4:4684. doi:10.1038/srep04684
47. Xie X, Zhou Y, Huang K. Advances in Microwave-Assisted Production of Reduced Graphene Oxide. *Front Chem.* **2019**;7. doi:10.3389/fchem.2019.00355



48. Park SH, Kim HS. Environmentally benign and facile reduction of graphene oxide by flash light irradiation. *Nanotechnology*. 2015;26(20):205601. doi:10.1088/0957-4484/26/20/205601
49. Voiry D, Yang J, Fullon R, et al. High-quality graphene via microwave reduction of solution-exfoliated graphene oxide. *Science*. 2016;353(6306):1413–1416. doi:10.1126/science.aah3398
50. Shao Y, Wang J, Engelhard M, Wang C, Lin Y. Facile and controllable electrochemical reduction of graphene oxide and its applications. *J Mater Chem*. 2010;20(4):743–748. doi:10.1039/B917975E
51. Zhou A, Bai J, Hong W, Bai H. Electrochemically reduced graphene oxide: preparation, composites, and applications. *Carbon*. 2022;191:301–332.
52. Gao M, Xu Y, Wang X, Sang Y, Wang S. Analysis of Electrochemical Reduction Process of Graphene Oxide and its Electrochemical Behavior. *Electroanalysis*. 2016;28(6):1377–1382. doi:10.1002/elan.201501063
53. Chen L, Tang Y, Wang K, Liu C, Luo S. Direct electrodeposition of reduced graphene oxide on glassy carbon electrode and its electrochemical application. *Electrochem Commun*. 2011;13(2):133–137. doi:10.1016/j.elecom.2010.11.033
54. Chua CK, Pumera M, Pumera M. chemical reduction of graphene oxide: a synthetic chemistry viewpoint. *Chem Soc Rev*. 2014;43:291–312. doi:10.1039/C3CS60303B
55. Lin Q, Zhang J, Lv W, et al. A functionalized carbon surface for high-performance sodium-ion storage. *Small*. 2020;16(15):1902603. doi:10.1002/sml.201902603
56. Qiu Y, Park K. Environment-sensitive hydrogels for drug delivery. *Adv Drug Deliv Rev*. 2001;53(3):321–339. doi:10.1016/S0169-409X(01)00203-4
57. Biswas MC, Islam MT, Nandy PK, Hossain MM. Graphene Quantum Dots (GQDs) for Bioimaging and Drug Delivery Applications: a Review. *ACS Mater Lett*. 2021;3(6):889–911. doi:10.1021/acsmaterialslett.0c00550
58. Zaini MS, Ying Chyi Liew J, Alang Ahmad SA, Mohmad AR, Kamarudin MA. Quantum Confinement Effect and Photoenhancement of Photoluminescence of PbS and PbS/MnS Quantum Dots. *Appl Sci*. 2020;10(18):6282. doi:10.3390/app10186282
59. Hernandez Y, Nicolosi V, Lotya M, et al. High-yield production of graphene by liquid-phase exfoliation of graphite. *Nat Nanotechnol*. 2008;3(9):563–568. doi:10.1038/nnano.2008.215
60. O'Neill A, Khan U, Nirmalraj PN, Boland J, Coleman JN. Graphene Dispersion and Exfoliation in Low Boiling Point Solvents. *J Phys Chem C*. 2011;115(13):5422–5428. doi:10.1021/jp110942e
61. Arao Y, Kuwahara R, Ohno K, et al. Mass production of low-boiling point solvent- and water-soluble graphene by simple salt-assisted ball milling. *Nanoscale Adv*. 2019;1(12):4955–4964. doi:10.1039/C9NA00463G
62. Azimi Z, Alimohammadian M, Sohrabi B. Graphene Quantum Dots Based on Mechanical Exfoliation Methods: a Simple and Eco-Friendly Technique. *ACS Omega*. 2024;9(29):31427–31437. doi:10.1021/acsomega.4c00453
63. Shanmugapriya V, Bharathi S, Esakkinaveen D, et al. Structural, Optical, and Magnetic Properties of Gd Doped CdTe Quantum Dots for Magnetic Imaging Applications. *ECS J Solid State Sci Technol*. 2022;11:1.
64. Gao H, Xue C, Hu G, Zhu K. Production of graphene quantum dots by ultrasound-assisted exfoliation in supercritical CO<sub>2</sub>/H<sub>2</sub>O medium. *Ultrason Sonochem*. 2017;37:120–127. doi:10.1016/j.ultsonch.2017.01.001
65. Bader KB, Raymond JL, Mobley J, Church CC, Felipe Gaitan D. The effect of static pressure on the inertial cavitation threshold. *J Acoust Soc Am*. 2012;132(2):728–737. doi:10.1121/1.4733539
66. Luo P, Guan X, Yu Y, Li X, Yan F. Hydrothermal Synthesis of Graphene Quantum Dots Supported on Three-Dimensional Graphene for Supercapacitors. *Nanomaterials*. 2019;9(2):201. doi:10.3390/nano9020201
67. He J, Li Z, Lu Y, et al. Aqueous synthesis of amphiphilic graphene quantum dots and their application as surfactants for preparing of fluorescent polymer microspheres. *Colloids Surf A*. 2018;563:1.
68. Li Y, Li Y, Wang J, et al. Electrochemical synthesis of phosphorus-doped graphene quantum dots for free radical scavenging. *Phys Chem Chem Phys*. 2017;19(18):11631–11638. doi:10.1039/C6CP06377B
69. Lee J, Kim K, Park WI, et al. Uniform graphene quantum dots patterned from self-assembled silica nanodots. *Nano Lett*. 2012;12(12):6078–6083. doi:10.1021/nl302520m
70. Kang SH, Mhin S, Han H, et al. Ultrafast Method for Selective Design of Graphene Quantum Dots with Highly Efficient Blue Emission. *Sci Rep*. 2016;6(1):38423. doi:10.1038/srep38423
71. Calabro RL, Yang DS, Kim DY. Liquid-phase laser ablation synthesis of graphene quantum dots from carbon nano-onions: comparison with chemical oxidation. *J Colloid Interface Sci*. 2018;527:132–140. doi:10.1016/j.jcis.2018.04.113
72. Zhuo S, Shao M, Lee ST. Upconversion and downconversion fluorescent graphene quantum dots: ultrasonic preparation and photocatalysis. *ACS Nano*. 2012;6(2):1059–1064. doi:10.1021/nn2040395
73. Kortel M, Mansuriya BD, Vargas Santana N, Altintas Z. Graphene Quantum Dots as Flourishing Nanomaterials for Bio-Imaging, Therapy Development, and Micro-Supercapacitors. *Micromachines*. 2020;11(9):866. doi:10.3390/mi11090866
74. Tian P, Tang L, Teng KS, Lau SP. Graphene quantum dots from chemistry to applications. *Mater Today Chem*. 2018;10:221–258.
75. Su J, Zhang X, Yao F, Guo R, Yuan C. Preparation of graphene quantum dots with high quantum yield by a facile one-step method and applications for cell imaging. *Mater Lett*. 2020;271:127806. doi:10.1016/j.matlet.2020.127806
76. Danial WH, Norhisham NA, Ahmad Noorden AF, Abdul Majid Z, Matsumura K, Iqbal A. Iqbal A: a short review on electrochemical exfoliation of graphene and graphene quantum dots. *Carbon Lett*. 2021;31(3):371–388. doi:10.1007/s42823-020-00212-3
77. Cao Y, Dong H, Yang Z, et al. Aptamer-Conjugated Graphene Quantum Dots/Porphyrin Derivative Theranostic Agent for Intracellular Cancer-Related MicroRNA Detection and Fluorescence-Guided Photothermal/Photodynamic Synergetic Therapy. *ACS Appl Mater Interfaces*. 2017;9(1):159–166. doi:10.1021/acsaami.6b13150
78. Zhao C, Song X, Liu Y, et al. Synthesis of graphene quantum dots and their applications in drug delivery. *J Nanobiotechnol*. 2020;18(1):142. doi:10.1186/s12951-020-00698-z
79. Yang K, Feng L, Liu Z. Stimuli responsive drug delivery systems based on nano-graphene for cancer therapy. *Adv Drug Deliv Rev*. 2016;105:228–241. doi:10.1016/j.addr.2016.05.015
80. Mbeh DA, Akhavan O, Javanbakht T, Mahmoudi M, Yahia LH. Cytotoxicity of protein Corona-graphene oxide nanoribbons on human epithelial cells. *Appl Surf Sci*. 2014;320:596–601. doi:10.1016/j.apsusc.2014.09.155

81. Dimiev AM, Khannanov A, Vakhitov I, Kiiamov A, Shukhina K, Tour JM. Revisiting the Mechanism of Oxidative Unzipping of Multiwall Carbon Nanotubes to Graphene Nanoribbons. *ACS Nano*. 2018;12(4):3985–3993. doi:10.1021/acsnano.8b01617
82. Wang G, Yang J, Park J, et al. Facile Synthesis and Characterization of Graphene Nanosheets. *J Phys Chem C*. 2008;112(22):8192–8195. doi:10.1021/jp710931h
83. Li L, Xu J, Li G, et al. Preparation of graphene nanosheets by shear-assisted supercritical CO<sub>2</sub> exfoliation. *Chem Eng J*. 2016;284:78–84. doi:10.1016/j.cej.2015.08.077
84. Malina T, Maršáková E, Holá K, et al. Toxicity of graphene oxide against algae and cyanobacteria: nanoblade-morphology-induced mechanical injury and self-protection mechanism. *Carbon*. 2019;155:386–396. doi:10.1016/j.carbon.2019.08.086
85. Shao X, Fang Z, Li M, et al. Graphene Oxide Nanosheets Induce Mitochondrial Fragmentation by Cutting through Membrane. *ACS Mater Lett*. 2023;5(9):2308–2316. doi:10.1021/acsmaterialslett.3c00177
86. Akhavan O, Ghaderi E, Akhavan A. Size-dependent genotoxicity of graphene nanoplatelets in human stem cells. *Biomaterials*. 2012;33(32):8017–8025. doi:10.1016/j.biomaterials.2012.07.040
87. Su Z, Chen W, Liang S, et al. Multifaceted Characterization for the Hepatic Clearance of Graphene Oxide and Size-Related Hepatic Toxicity. *Molecules*. 2024;29(6):1335. doi:10.3390/molecules29061335
88. Zvyagina AI, Alexandrov AE, Averin AA, et al. One-Step Interfacial Integration of Graphene Oxide and Organic Chromophores into Multicomponent Nanohybrids with Photoelectric Properties. *Langmuir*. 2022;38(49):15145–15155. doi:10.1021/acs.langmuir.2c02155
89. Zhang J, Liu D, Ou Q, Lu Y, Huang J. Covalent Coupling of Porphyrins with Monolayer Graphene for Low-Voltage Synaptic Transistors. *ACS Appl Mater Interfaces*. 2022;14(9):11699–11707. doi:10.1021/acsami.1c22073
90. Li D, He X, Zhao L, et al. Ultrafast Electron Transfer Dynamics of Organic Polymer Nanoparticles with Graphene Oxide. *Chemistry*. 2023;29(22):e202300025. doi:10.1002/chem.202300025
91. Shashikala HM, Nicolas CI, Wang X-Q. Tunable doping in graphene by light-switchable molecules. *J Phys Chem C*. 2012;116(49):26102–26105. doi:10.1021/jp311269c
92. Wang A, Yu W, Huang Z, et al. Covalent functionalization of reduced graphene oxide with porphyrin by means of diazonium chemistry for nonlinear optical performance. *Sci Rep*. 2016;6(1):23325. doi:10.1038/srep23325
93. Dash BS, Lu Y-J, Chen J-P. Enhancing Photothermal/Photodynamic Therapy for Glioblastoma by Tumor Hypoxia Alleviation and Heat Shock Protein Inhibition Using IR820-Conjugated Reduced Graphene Oxide Quantum Dots. *ACS Appl Mater Interfaces*. 2024;16(11):13543–13562. doi:10.1021/acsami.3c19152
94. Yu XT, Sui SY, He YX, Yu CH, Peng Q. Nanomaterials-based photosensitizers and delivery systems for photodynamic cancer therapy. *Biomater Adv*. 2022;135:212725. doi:10.1016/j.bioadv.2022.212725
95. Aires-Fernandes M, Botelho Costa R, Rochetti Do Amaral S, Mussagy CU, Santos-Ebinuma VC, Primo FL. Development of Biotechnological Photosensitizers for Photodynamic Therapy: cancer Research and Treatment-From Benchtop to Clinical Practice. *Molecules*. 2022;27(20):6848. doi:10.3390/molecules27206848
96. Bartusik-Aebischer D, Woźnicki P, Dynarowicz K, Aebischer D. Photosensitizers for Photodynamic Therapy of Brain Cancers—A Review. *Brain Sciences*. 2023;13(9):1299. doi:10.3390/brainsci13091299
97. Wooten RS, Smith KC, Ahlquist DA, Muller SA, Balm RK. Prospective study of cutaneous phototoxicity after systemic hematoporphyrin derivative. *Lasers Surg Med*. 1988;8(3):294–300. doi:10.1002/lsm.1900080312
98. Gunaydin G, Gedik ME, Ayan S. Photodynamic Therapy for the Treatment and Diagnosis of Cancer-A Review of the Current Clinical Status. *Front Chem*. 2021;9. doi:10.3389/fchem.2021.686303
99. Wang S-B, Chen Z-X, Gao F, et al. Remodeling extracellular matrix based on functional covalent organic framework to enhance tumor photodynamic therapy. *Biomaterials*. 2020;234:119772. doi:10.1016/j.biomaterials.2020.119772
100. Beharry AA. Next-Generation Photodynamic Therapy: new Probes for Cancer Imaging and Treatment. *Biochemistry*. 2018;57(2):173–174. doi:10.1021/acs.biochem.7b01037
101. Li X, Wang X, Gu J, Ma Y, Liu Z, Shi Y. Needle-free injection of 5-aminolevulinic acid in photodynamic therapy for the treatment of condylomata acuminata. *Exp Ther Med*. 2013;6(1):236–240. doi:10.3892/etm.2013.1092
102. Longmire M, Choyke PL, Kobayashi H. Clearance properties of nano-sized particles and molecules as imaging agents: considerations and caveats. *Nanomedicine*. 2008;3(5):703–717. doi:10.2217/17435889.3.5.703
103. Brozek-Pluska B, Jarota A, Kania R, Abramczyk H. Abramczyk H: zinc Phthalocyanine Photochemistry by Raman Imaging, Fluorescence Spectroscopy and Femtosecond Spectroscopy in Normal and Cancerous Human Colon Tissues and Single Cells. *Molecules*. 2020;25(11):2688. doi:10.3390/molecules25112688
104. Chilakamarthi U, Giribabu L. Photodynamic Therapy: past, Present and Future. *Chem Rec*. 2017;17(8):775–802. doi:10.1002/tcr.201600121
105. D'Alessandro S, Priefer R. Non-porphyrin dyes used as photosensitizers in photodynamic therapy. *J Drug Delivery Sci Technol*. 2020;60:101979. doi:10.1016/j.jddst.2020.101979
106. Lan G, Ni K, Xu Z, Veroneau SS, Song Y, Lin W. Nanoscale Metal–Organic Framework Overcomes Hypoxia for Photodynamic Therapy Primed Cancer Immunotherapy. *J Am Chem Soc*. 2018;140(17):5670–5673. doi:10.1021/jacs.8b01072
107. Li J, Li Y, Chen P. Biological mediated synthesis of reduced graphene oxide (rGO) as a potential electron shuttle for facilitated biological denitrification: insight into the electron transfer process. *J Environ Chem Eng*. 2022;10(5):108225. doi:10.1016/j.jece.2022.108225
108. Fan HY, X-h Y, Wang K, Y-j Y, Tang Y-j, Tang Y-l, Liang X-h: graphene quantum dots (GQDs)-based nanomaterials for improving photodynamic therapy in cancer treatment. *Eur. J. Med Chem*. 2019;182:111620. doi:10.1016/j.ejmech.2019.111620
109. BL L, Li R, HL Z, Ariga K, NB L, Leong DT. Engineered functionalized 2D nanoarchitectures for stimuli-responsive drug delivery. *Mater Horizons*. 2020;7(2):455–469. doi:10.1039/C9MH01300H
110. Brancalion L, Moseley H. Laser and non-laser light sources for photodynamic therapy. *Lasers Med Sci*. 2002;17(3):173–186. doi:10.1007/s101030200027
111. Mang TS. Lasers and light sources for PDT: past, present and future. *Photodiagnosis Photodyn Ther*. 2004;1(1):43–48. doi:10.1016/S1572-1000(04)00012-2
112. Kim MM, Darafsheh A. Light sources and dosimetry techniques for photodynamic therapy. *Photochem Photobiol*. 2020;96(2):280–294. doi:10.1111/php.13219

113. Profio A, Doiron D. Transport of light in tissue in photodynamic therapy. *Photochem Photobiol.* **1987**;46(5):591–599. doi:10.1111/j.1751-1097.1987.tb04819.x
114. Algorri JF, Ochoa M, Roldán-Varona P, Rodríguez-Cobo L, López-Higuera JM. Light Technology for Efficient and Effective Photodynamic Therapy: a Critical Review. *Cancers.* **2021**;13(14):3484. doi:10.3390/cancers13143484
115. Fan W, Huang P, Chen X. Overcoming the Achilles' heel of photodynamic therapy. *Chem Soc Rev.* **2016**;45(23):6488–6519. doi:10.1039/C6CS00616G
116. Jacques SL. How tissue optics affect dosimetry of photodynamic therapy. *J Biomed Opt.* **2010**;15(5):051608–051608–051606. doi:10.1117/1.3494561
117. Etcheverry ME, Pasquale MA, Garavaglia M. Photodynamic therapy of HeLa cell cultures by using LED or laser sources. *J Photochem Photobiol B Biol.* **2016**;160:271–277. doi:10.1016/j.jphotobiol.2016.04.013
118. Reddy MLP, Bejyomohandas KS. Evolution of 2, 3'-bipyridine class of cyclometalating ligands as efficient phosphorescent iridium(III) emitters for applications in organic light emitting diodes. *J Photochem Photobiol C Photochem Rev.* **2016**;29:29–47. doi:10.1016/j.jphotochemrev.2016.10.001
119. Turan IS, Yildiz D, Turksoy A, Gunaydin G, Akkaya EU. Akkaya EU: a Bifunctional Photosensitizer for Enhanced Fractional Photodynamic Therapy: singlet Oxygen Generation in the Presence and Absence of Light. *Angew Chem Int Ed Engl.* **2016**;55(8):2875–2878. doi:10.1002/anie.201511345
120. Rodrigues JA, Correia JH. Photodynamic Therapy for Colorectal Cancer: an Update and a Look to the Future. *Int J Mol Sci.* **2023**;24(15):12204. doi:10.3390/ijms241512204
121. Chen D, Shen Y, Huang Z, Li B, Xie S. Light-emitting diode based illumination system for in vitro photodynamic therapy. *Photodiagn Photodyn Ther.* **2011**;8(2):200. doi:10.1016/j.pdpdt.2011.03.256
122. Yoon I, Li JZ, Shim YK. Advance in Photosensitizers and Light Delivery for Photodynamic Therapy. *Clin Endosc.* **2013**;46(1):7–23. doi:10.5946/ce.2013.46.1.7
123. Li X, Lovell JF, Yoon J, Chen X. Clinical development and potential of photothermal and photodynamic therapies for cancer. *Nat Rev Clin Oncol.* **2020**;17(11):657–674. doi:10.1038/s41571-020-0410-2
124. Hu J, Tang Y, Elmenoufy AH, Cheng Z, Yang X, Yang X. Nanocomposite-Based Photodynamic Therapy Strategies for Deep Tumor Treatment. *Small.* **2015**;11(44):5860–5887. doi:10.1002/smll.201501923
125. He XJ, Aker WG, Huang MJ, Watts JD, Hwang HM. Metal Oxide Nanomaterials in Nanomedicine: applications in Photodynamic Therapy and Potential Toxicity. *Curr Top Med Chem.* **2015**;15(18):1887–1900. doi:10.2174/1568026615666150506145251
126. Qi F, Chang Y, Zheng RX, et al. Copper Phosphide Nanoparticles Used for Combined Photothermal and Photodynamic Tumor Therapy. *ACS Biomater Sci Eng.* **2021**;7:2745–2754.
127. Huang Y, Qiu F, Chen R, Yan D, Zhu X. Fluorescence resonance energy transfer-based drug delivery systems for enhanced photodynamic therapy. *J Mater Chem B.* **2020**;8(17):3772–3788. doi:10.1039/D0TB00262C
128. Li B, Lin L. Internal light source for deep photodynamic therapy. *Light Sci Appl.* **2022**;11(1):85. doi:10.1038/s41377-022-00780-1
129. Mroz P, Yaroslavsky A, Kharkwal GB, Hamblin MR. Cell death pathways in photodynamic therapy of cancer. *Cancers.* **2011**;3(2):2516–2539. doi:10.3390/cancers3022516
130. Felsner DW. Cancer revoked: oncogenes as therapeutic targets. *Nat Rev Cancer.* **2003**;3(5):375–380. doi:10.1038/nrc1070
131. Correia JH, Rodrigues JA, Pimenta S, Dong T, Yang Z. Photodynamic Therapy Review: principles, Photosensitizers, Applications, and Future Directions. *Pharmaceutics.* **2021**;13(9):1332. doi:10.3390/pharmaceutics13091332
132. Agostinis P, Berg K, Cengel KA, et al. Photodynamic therapy of cancer: an update. *CA Cancer J Clin.* **2011**;61(4):250–281. doi:10.3322/caac.20114
133. Yoo JO, Ha KS. New insights into the mechanisms for photodynamic therapy-induced cancer cell death. *Int Rev Cell Mol Biol.* **2012**;295:139–174.
134. Allison RR, Moghissi K. Oncologic photodynamic therapy: clinical strategies that modulate mechanisms of action. *Photodiagnosis Photodyn Ther.* **2013**;10(4):331–341. doi:10.1016/j.pdpdt.2013.03.011
135. Igney FH, Krammer PH. Death and anti-death: tumour resistance to apoptosis. *Nat Rev Cancer.* **2002**;2(4):277–288. doi:10.1038/nrc776
136. Rathmell JC, Thompson CB. The central effectors of cell death in the immune system. *Annu Rev Immunol.* **1999**;17(1):781–828. doi:10.1146/annurev.immunol.17.1.781
137. Savill J, Fadok V. Corpse clearance defines the meaning of cell death. *Nature.* **2000**;407(6805):784–788. doi:10.1038/35037722
138. Lavrik I, Golks A, Krammer PH. Death receptor signaling. *J Cell Sci.* **2005**;118(2):265–267. doi:10.1242/jcs.01610
139. Yuan Z, Dewson G, Czabotar PE, Birkinshaw RW. VDAC2 and the BCL-2 family of proteins. *Biochem Soc Trans.* **2021**;49(6):2787–2795. doi:10.1042/BST20210753
140. Mesquita MQ, Ferreira AR, Neves M, Ribeiro D, Fardilha M, Faustino MAF. Photodynamic therapy of prostate cancer using porphyrinic formulations. *J Photochem Photobiol B.* **2021**;223:112301. doi:10.1016/j.jphotobiol.2021.112301
141. Girotti AW. Photodynamic lipid peroxidation in biological systems. *Photochem Photobiol.* **1990**;51(4):497–509. doi:10.1111/j.1751-1097.1990.tb01744.x
142. Girotti AW. Photosensitized oxidation of cholesterol in biological systems: reaction pathways, cytotoxic effects and defense mechanisms. *J Photochem Photobiol B Biol.* **1992**;13(2):105–118. doi:10.1016/1011-1344(92)85050-5
143. Li G, Wang Q, Liu J, et al. Innovative strategies for enhanced tumor photodynamic therapy. *J Mater Chem B.* **2021**;9(36):7347–7370. doi:10.1039/D1TB01466H
144. Meng Z, Xue H, Wang T, et al. Aggregation-induced emission photosensitizer-based photodynamic therapy in cancer: from chemical to clinical. *J Nanobiotechnology.* **2022**;20(1):344. doi:10.1186/s12951-022-01553-z
145. Li WH, Weng XX, Yuan LF, Li F, Yue XP, Li FD. Effect of feeding linseed diet on testis development, antioxidant capacity, and epididymal cauda sperm concentration in Chinese Hu lamb. *Theriogenology.* **2021**;159:69–76. doi:10.1016/j.theriogenology.2020.10.014
146. Gołab J, Olszewska D, Mróz P, et al. Erythropoietin Restores the Antitumor Effectiveness of Photodynamic Therapy in Mice with Chemotherapy- induced Anemia1. *Clin Cancer Res.* **2002**;8(5):1265–1270.

147. Li W-P, Yen C-J, Wu B-S, Wong T-W. Recent Advances in Photodynamic Therapy for Deep-Seated Tumors with the Aid of Nanomedicine. *Biomedicines*. 2021;9(1):69. doi:10.3390/biomedicines9010069
148. Singh PP, Sinha S, Gahtori P, Mishra DN, Pandey G, Srivastava V. Recent advancement in photosensitizers for photodynamic therapy. *Dyes Pigm*. 2024;229:112262. doi:10.1016/j.dyepig.2024.112262
149. Kwiatkowski S, Knap B, Przysupski D, et al. Photodynamic therapy – mechanisms, photosensitizers and combinations. *Biomed Pharmacother*. 2018;106:1098–1107. doi:10.1016/j.biopha.2018.07.049
150. Ming L, Cheng K, Chen Y, Yang R, Chen D. Enhancement of tumor lethality of ROS in photodynamic therapy. *Cancer Med*. 2021;10(1):257–268. doi:10.1002/cam4.3592
151. Zhen Z, Zhu H. 1 - Structure and Properties of Graphene. In: Zhu H, Xu Z, Xie D, Fang Y, editors. *Graphene*. Academic Press; 2018:1–12.
152. Yang Q, Su Y, Chi C, et al. Ultrathin graphene-based membrane with precise molecular sieving and ultrafast solvent permeation. *Nature Mater*. 2017;16(12):1198–1202. doi:10.1038/nmat5025
153. Chen P, Yue H, Zhai X, et al. Transport of a graphene nanosheet sandwiched inside cell membranes. *Sci Adv*. 2019;5(6):eaaw3192. doi:10.1126/sciadv.aaw3192
154. Ibrahim A, Klopocinska A, Horvat K, Abdel Hamid Z. Graphene-Based Nanocomposites: synthesis, Mechanical Properties, and Characterizations. *Polymers*. 2021;13(17):2869. doi:10.3390/polym13172869
155. Nair RR, Blake P, Grigorenko AN, et al. Fine Structure Constant Defines Visual Transparency of Graphene. *Science*. 2008;320(5881):1308. doi:10.1126/science.1156965
156. Vejpravová J. Mixed sp<sup>2</sup>–sp<sup>3</sup> Nanocarbon Materials: a Status Quo Review. *Nanomaterials*. 2021;11(10):2469. doi:10.3390/nano11102469
157. Wu J, Jia L, Zhang Y, Qu Y, Jia B, Moss DJ. Graphene oxide for integrated photonics and flat optics. *Adv Mater*. 2021;33(3):2006415. doi:10.1002/adma.202006415
158. Jin Y, Zheng Y, Podkolzin SG, Lee W. Band gap of reduced graphene oxide tuned by controlling functional groups. *J Mater Chem C*. 2020;8(14):4885–4894. doi:10.1039/C9TC07063J
159. Wang X, Hu C, Gu Z, Dai L. Understanding of catalytic ROS generation from defect-rich graphene quantum-dots for therapeutic effects in tumor microenvironment. *J Nanobiotechnol*. 2021;19(1):340. doi:10.1186/s12951-021-01053-6
160. Mojgan R, Ehsan S, Mostafa Z. High photoluminescence and afterglow emission of nitrogen-doped graphene quantum dots/TiO<sub>2</sub> nanocomposite for use as a photodynamic therapy photosensitizer. *Appl Phys A*. 2024;130(3):144. doi:10.1007/s00339-024-07305-0
161. Wu Z, Xia W, Ou L, et al. Utilization of Nitrogen-Doped Graphene Quantum Dots to Neutralize ROS and Modulate Intracellular Antioxidant Pathways to Improve Dry Eye Disease Therapy. *Int J Nanomed*. 2024;19:2691–2708. doi:10.2147/IJN.S445398
162. Prabakaran G, Velmurugan K, David CI, Nandhakumar R. Role of Förster resonance energy transfer in graphene-based nanomaterials for sensing. *Appl Sci*. 2022;12(14):6844. doi:10.3390/app12146844
163. Dash BS, Lu Y-J, Pejrim P, Lan Y-H, Chen J-P. Hyaluronic acid-modified, IR780-conjugated and doxorubicin-loaded reduced graphene oxide for targeted cancer chemo/photothermal/photodynamic therapy. *Biomaterials Advances*. 2022;136:212764. doi:10.1016/j.bioadv.2022.212764
164. Yang Y, Cao J, Wei N, et al. Thermal Conductivity of Defective Graphene Oxide: a Molecular Dynamic Study. *Molecules*. 2019;24:2.
165. Bienia A, Wiecheć-Cudak O, Murzyn AA, Krzykawska-Serda M. Photodynamic Therapy and Hyperthermia in Combination Treatment—Neglected Forces in the Fight against Cancer. *Pharmaceutics*. 2021;13(8):1147. doi:10.3390/pharmaceutics13081147
166. Di Corato R, Béalle G, Kolosnjaj-Tabi J, et al. Combining magnetic hyperthermia and photodynamic therapy for tumor ablation with photoresponsive magnetic liposomes. *ACS Nano*. 2015;9(3):2904–2916. doi:10.1021/nn506949t
167. Tian B, Wang C, Zhang S, Feng L, Liu Z. Photothermally Enhanced Photodynamic Therapy Delivered by Nano-Graphene Oxide. *ACS Nano*. 2011;5(9):7000–7009. doi:10.1021/nn201560b
168. Liu Z, Robinson JT, Sun X, Dai H. PEGylated Nanographene Oxide for Delivery of Water-Insoluble Cancer Drugs. *J Am Chem Soc*. 2008;130(33):10876–10877. doi:10.1021/ja803688x
169. Bao H, Pan Y, Sahoo NG, Wu T, Gan LH. Chitosan-Functionalized Graphene Oxide as a Nanocarrier for Drug and Gene Delivery. *Small*. 2011;7(11):1569–1578. doi:10.1002/sml.201100191
170. Xia Y, Zhang H, Xu F, et al. Graphene-oxide-induced lamellar structures used to fabricate novel composite solid-solid phase change materials for thermal energy storage. *Chem Eng J*. 2019;362:909–920. doi:10.1016/j.cej.2019.01.097
171. Feng S, Zhao Q, Mu X. Mesoporous carbon nanoenzyme as nano-booster for photothermal-enhanced photodynamic therapy compared with graphene oxide. *Colloids Surf B Biointerfaces*. 2023;222:113095. doi:10.1016/j.colsurfb.2022.113095
172. Sun X, Zebibula A, Dong X, Qian J, He S. Aggregation-Induced Emission Nanoparticles Encapsulated with PEGylated Nano Graphene Oxide and Their Applications in Two-Photon Fluorescence Bioimaging and Photodynamic Therapy in Vitro and in Vivo. *ACS Appl Mater Interfaces*. 2018;10(30):25037–25046. doi:10.1021/acsami.8b05546
173. Liu F, Xu C, Li J, Zhang Z, Jin X, Wang B. Nanoarchitectonics of versatile platform based on graphene oxide for precise and enhanced synergistic cancer photothermal-photodynamic/chemotherapy. *J Mol Struct*. 2023;1294:136499. doi:10.1016/j.molstruc.2023.136499
174. Ledermann J, Canevari S, Thigpen T. Targeting the folate receptor: diagnostic and therapeutic approaches to personalize cancer treatments. *Ann Oncol*. 2015;26(10):2034–2043. doi:10.1093/annonc/mdv250
175. Huang P, Xu C, Lin J, et al. Folic Acid-conjugated Graphene Oxide loaded with Photosensitizers for Targeting Photodynamic Therapy. *Theranostics*. 2011;1:240–250. doi:10.7150/thno.v01p0240
176. Yang K, Sun X, Lee ST, Liu Z, Lee S-T, Liu Z. Graphene in mice: ultrahigh in vivo tumor uptake and efficient photothermal therapy. *Nano Lett*. 2010;10(9):3318–3323. doi:10.1021/nl100996u
177. Shahnawaz Khan M, Abdelhamid HN, Wu H-F. Near infrared (NIR) laser mediated surface activation of graphene oxide nanoflakes for efficient antibacterial, antifungal and wound healing treatment. *Colloids Surf B*. 2015;127:281–291. doi:10.1016/j.colsurfb.2014.12.049
178. Kalluru P, Vankayala R, Chiang C-S, Hwang KC. Nano-graphene oxide-mediated In vivo fluorescence imaging and bimodal photodynamic and photothermal destruction of tumors. *Biomaterials*. 2016;95:1–10. doi:10.1016/j.biomaterials.2016.04.006
179. Li Y, Dong H, Li Y, Shi D. Graphene-based nanovehicles for photodynamic medical therapy. *Int J Nanomed*. 2015;10:2451–2459. doi:10.2147/IJN.S68600
180. Huang P, Wang S, Wang X, et al. Surface Functionalization of Chemically Reduced Graphene Oxide for Targeted Photodynamic Therapy. *J Biomed Nanotechnol*. 2015;11(1):117–125. doi:10.1166/jbn.2015.2055



181. Ma W, Yang H, Hu Y, Chen L. Fabrication of PEGylated porphyrin/reduced graphene oxide/doxorubicin nanoplatfor for tumour combination therapy. *Poly Int*. 2021;70(9):1413–1420. doi:10.1002/pi.6216
182. Vinothini K, Rajendran NK, Mariappan R, Andy R, Marraiki N, Elgorban AM. A magnetic nanoparticle functionalized reduced graphene oxide-based drug carrier system for a chemo-photodynamic cancer therapy. *New J Chem*. 2020;44(14):5265–5277. doi:10.1039/D0NJ00049C
183. Kadkhoda J, Tarighatnia A, Barar J, Aghanejad A, Davaran S. Recent advances and trends in nanoparticles based photothermal and photodynamic therapy. *Photodiagnosis Photodyn Ther*. 2022;37:102697. doi:10.1016/j.pdpdt.2021.102697
184. Jiang W, Mo F, Jin X, et al. Tumor-Targeting Photothermal Heating-Responsive Nanoplatfor Based on Reduced Graphene Oxide/Mesoporous Silica/Hyaluronic Acid Nanocomposite for Enhanced Photodynamic Therapy. *Adv Mater Interfaces*. 2017;4(20):1700425. doi:10.1002/admi.201700425
185. Shuvra Smita S, Das A, Barui A. Surface Functionalization of Green-synthesized Reduced Graphene Oxide with PPIX Enhances Photosensitization of Cancer Cells. *Photochem Photobiol*. 2020;96(6):1283–1293. doi:10.1111/php.13316
186. Dash BS, Jose G, Lu YJ, Chen JP. Functionalized Reduced Graphene Oxide as a Versatile Tool for Cancer Therapy. *Int J Mol Sci*. 2021;22(6):2989. doi:10.3390/ijms22062989
187. Huang W-T, Chan M-H, Chen X, Hsiao M, Liu R-S. Theranostic nanobubble encapsulating a plasmon-enhanced upconversion hybrid nanosystem for cancer therapy. *Theranostics*. 2020;10(2):782–796. doi:10.7150/thno.38684
188. Wang X, Li Z, Ding Y, et al. Enhanced photothermal-photodynamic therapy for glioma based on near-infrared dye functionalized Fe<sub>3</sub>O<sub>4</sub> superparticles. *Chem Eng J*. 2020;381:122693. doi:10.1016/j.cej.2019.122693
189. Ibrahim M, Ramadan E, Elsadek NE, et al. Polyethylene glycol (PEG): the nature, immunogenicity, and role in the hypersensitivity of PEGylated products. *J Control Release*. 2022;351:215–230. doi:10.1016/j.jconrel.2022.09.031
190. Melo BL, Lima-Sousa R, Alves CG, Correia IJ, De melo-diogo D. Sulfobetaine methacrylate-coated reduced graphene oxide-IR780 hybrid nanosystems for effective cancer photothermal-photodynamic therapy. *Int J Pharm*. 2023;647:123552. doi:10.1016/j.ijpharm.2023.123552
191. Men Y, Peng S, Yang P, et al. Biodegradable Zwitterionic Nanogels with Long Circulation for Antitumor Drug Delivery. *ACS Appl Mater Interfaces*. 2018;10(28):23509–23521. doi:10.1021/acsami.8b03943
192. Markovic ZM, Ristic BZ, Arsiokin KM, et al. Graphene quantum dots as autophagy-inducing photodynamic agents. *Biomaterials*. 2012;33(29):7084–7092. doi:10.1016/j.biomaterials.2012.06.060
193. Ge J, Lan M, Zhou B, et al. A graphene quantum dot photodynamic therapy agent with high singlet oxygen generation. *Nat Commun*. 2014;5(1):4596. doi:10.1038/ncomms5596
194. Ghaffarkhah A, Hosseini E, Kamkar M, et al. Synthesis, Applications, and Prospects of Graphene Quantum Dots: a Comprehensive Review. *Small*. 2022;18(2):e2102683. doi:10.1002/sml.202102683
195. Chung S, Revia RA, Zhang M. Graphene Quantum Dots and Their Applications in Bioimaging, Biosensing, and Therapy. *Adv Mater*. 2021;33(22):e1904362. doi:10.1002/adma.201904362
196. Wang D, Zhu L, Chen JF, Dai L. Can graphene quantum dots cause DNA damage in cells? *Nanoscale*. 2015;7(21):9894–9901. doi:10.1039/C5NR01734C
197. Mousavi SM, Kalashgrani MY, Javanmardi N, et al. Recent breakthroughs in graphene quantum dot-enhanced sonodynamic and photodynamic therapy. *J Mater Chem B*. 2024;12(29):7041–7062. doi:10.1039/D4TB00767K
198. Du D, Wang K, Wen Y, Li Y, YY L. Photodynamic Graphene Quantum Dot: reduction Condition Regulated Photoactivity and Size Dependent Efficacy. *ACS Appl Mater Interfaces*. 2016;8(5):3287–3294. doi:10.1021/acsami.5b11154
199. Chan M-H, Chen S-P, Chen C-W, et al. Single 808 nm Laser Treatment Comprising Photothermal and Photodynamic Therapies by Using Gold Nanorods Hybrid Upconversion Particles. *J Phys Chem C*. 2018;122(4):2402–2412. doi:10.1021/acs.jpcc.7b10976
200. Anjusha AJ, Thirunavukkarasu S, Resmi AN, Dhanapandian S, Krishnakumar N, Krishnakumar N. Multifunctional amino functionalized graphene quantum dots wrapped upconversion nanoparticles for photodynamic therapy and X-ray CT imaging. *Inorg Chem Commun*. 2023;149:110428. doi:10.1016/j.inoche.2023.110428
201. Mushtaq S, Yasin T, Saleem M, Dai T, Yameen MA. Potentiation of Antimicrobial Photodynamic Therapy by Curcumin-loaded Graphene Quantum Dots. *Photochemistry and Photobiology*. 2022;98(1):202–210. doi:10.1111/php.13503
202. Some S, Gwon AR, Hwang E, et al. Cancer Therapy Using Ultrahigh Hydrophobic Drug-Loaded Graphene Derivatives. *Sci Rep*. 2014;4(1):6314. doi:10.1038/srep06314
203. Yang Y, Wang B, Zhang X, et al. Activatable Graphene Quantum-Dot-Based Nanotransformers for Long-Period Tumor Imaging and Repeated Photodynamic Therapy. *Adv Mater*. 2023;35(23):e2211337. doi:10.1002/adma.202211337
204. Zarepour A, Khosravi A, Yücel Ayten N, Çakır Hatir P, Iravani S, Zarrabi A. Innovative approaches for cancer treatment: graphene quantum dots for photodynamic and photothermal therapies. *J Mater Chem B*. 2024;12(18):4307–4334. doi:10.1039/D4TB00255E
205. Pan D, Zhang J, Li Z, Wu M. Hydrothermal route for cutting graphene sheets into blue-luminescent graphene quantum dots. *Adv Mater*. 2010;22(6):734–738. doi:10.1002/adma.200902825
206. Liu G, Zhao P, Liu N, et al. Photosensitizer and anticancer drug-loaded 2D nanosheet: preparation, stability and anticancer property. *2D Mater*. 2019;6(4):045035. doi:10.1088/2053-1583/ab377b
207. Magdalan C, Elayaperumal M, Muthurulandi, Lachumananandasivam R, Neelamani S, Maaza M. Well-Aligned Graphene Oxide Nanosheets Decorated with Zinc Oxide Nanocrystals for High Performance Photocatalytic Application. *Int J Nanosci*. 2015;14:150125201131009.
208. Kiran HC, Gangadharappa HV. Reinforcing nanomedicine using graphene nanoribbons. *J Drug Delivery Sci Technol*. 2019;49:334–344. doi:10.1016/j.jddst.2018.12.004
209. Charmi J, Nosrati H, Mostafavi Amjad J, Mohammadkhani R, Danafar H. Polyethylene glycol (PEG) decorated graphene oxide nanosheets for controlled release curcumin delivery. *Heliyon*. 2019;5(4):e01466. doi:10.1016/j.heliyon.2019.e01466
210. Singh D. Graphene-tethered peptide nanosheets - A facile approach for cargo molecules in cancer. *Nano-Struct Nano-Objects*. 2024;37:101115. doi:10.1016/j.nanoso.2024.101115
211. Liu P, Xie X, Liu M, Hu S, Ding J, Zhou W. A smart MnO<sub>2</sub>-doped graphene oxide nanosheet for enhanced chemo-photodynamic combinatorial therapy via simultaneous oxygenation and glutathione depletion. *Acta Pharmaceutica Sinica B*. 2021;11(3):823–834. doi:10.1016/j.apsb.2020.07.021

212. Guo W, Chen Z, Feng X, et al. Graphene oxide (GO)-based nanosheets with combined chemo/photothermal/photodynamic therapy to overcome gastric cancer (GC) paclitaxel resistance by reducing mitochondria-derived adenosine-triphosphate (ATP). *J Nanobiotechnology*. 2021;19(1):146. doi:10.1186/s12951-021-00874-9
213. Hosseinzadeh R, Khorsandi K, Hosseinzadeh G. Graphene oxide-methylene blue nanocomposite in photodynamic therapy of human breast cancer. *J Biomol Struct Dyn*. 2018;36(9):2216–2223. doi:10.1080/07391102.2017.1345698
214. Lu H, Li W, Qiu P, et al. MnO<sub>2</sub> doped graphene nanosheets for carotid body tumor combination therapy. *Nanoscale Adv*. 2022;4:4304–4313. doi:10.1039/D2NA00086E
215. Abid SP, Islam SS, Mishra P, Ahmad S, Ahmad S. Reduced graphene oxide (rGO) based wideband optical sensor and the role of Temperature, Defect States and Quantum Efficiency. *Sci Rep*. 2018;8(1):3537. doi:10.1038/s41598-018-21686-2

### International Journal of Nanomedicine

### Publish your work in this journal

The International Journal of Nanomedicine is an international, peer-reviewed journal focusing on the application of nanotechnology in diagnostics, therapeutics, and drug delivery systems throughout the biomedical field. This journal is indexed on PubMed Central, MedLine, CAS, SciSearch®, Current Contents®/Clinical Medicine, Journal Citation Reports/Science Edition, EMBase, Scopus and the Elsevier Bibliographic databases. The manuscript management system is completely online and includes a very quick and fair peer-review system, which is all easy to use. Visit <http://www.dovepress.com/testimonials.php> to read real quotes from published authors.

Submit your manuscript here: <https://www.dovepress.com/international-journal-of-nanomedicine-journal>

**Dovepress**  
Taylor & Francis Group